# Dalton Transactions

Accepted Manuscript






ROYAL SOCIETY OF CHEMISTRY

www.rsc.org/dalton

Journal Name

ARTICLE

# Aluminum Methyl, Alkoxide and α-Alkoxy Ester Complexes Supported by 6,6'-Dimethylbiphenyl-Bridged Salen Ligands: Synthesis, Characterization and Catalysis for *rac*-Lactide Polymerization

Received 00th January 20xx,
Accepted 00th January 20xx

DOI: 10.1039/x0xx00000x

www.rsc.org/

Chao Kan, Jilei Ge and Haiyan Ma*

The synthesis and characterization of aluminum alkyl and alkoxide complexes bearing racemic 6,6'-dimethylbiphenyl-bridged salen-type ligands, and their catalysis in the ring-opening polymerization (ROP) of *rac*-lactide are reported. Reactions of $AlMe_3$ with various amounts of the proligands $\mathbf{L^{1-4}H_2}$ (6,6'-[(6,6'-dimethyl-[1,1'-biphenyl]-2,2'-diyl)bis(nitrylomethylidyne)]-bis(2-$R^1$-4-$R^2$-phenol): $\mathbf{L^1H_2}$, $R^1 = R^2$ = Me; $\mathbf{L^2H_2}$, $R^1$ = $^t$Bu, $R^2$ = Me; $\mathbf{L^3H_2}$, $R^1 = R^2$ = cumyl; $\mathbf{L^4H_2}$, $R^1$ = Br, $R^2$ = $^t$Bu) afforded the corresponding mono- and dinuclear aluminum methyl complexes [$\mathbf{L^{1-3}}$AlMe (**1**–**3**), $\mathbf{L^{1-4}}Al_2Me_4$ (**4**–**7**)]. Aluminum alkoxide complexes $\mathbf{L^2}$Al$^i$Pr (**8**), $\mathbf{L^2}$AlOBn (**9**), and α-alkoxy ester complexes $\mathbf{L^2}$Al(OCMe$_2$CO$_2$Me) (**10**), $\mathbf{L^2}$Al[(*S*)-OCHMeCO$_2$Me] (**11**) were prepared via *in situ* alcoholysis of the parent aluminum methyl complex **2** with the corresponding alcohols. The molecular structures of mononuclear complexes **1**–**3**, dinuclear complex **6**, alkoxide complexes **8**-**9** and α-alkoxy ester complexes **10**-**11** were established by single-crystal X-ray diffraction studies. Two broad resonances at about 69−70 ppm and 25−41 ppm were observed in the $^{27}$Al NMR spectra of complexes **10** and **11**, indicating the existence of both four- and five-coordinate aluminum centers in solution, which is resulted from the dissociation of one N donor of the salen ligand, accompanied by an association and dissociation equilibrium of the carbonyl group of the α-alkoxy ester ligand to the aluminum center. Complex **11** is also a rare example of *O*-lactate model complex that mimics the first insertion of *L*-LA. All complexes were investigated for the ROP of *rac*-LA at 110 °C in toluene. The polymerization initiated by complexes **1**–**3** in the presence of $^i$PrOH showed living features, affording PLAs with narrow molecular weight distributions (PDIs = 1.03–1.05) and 65−73% isotacticities. Particularly, complex **8** showed an "immortal" behavior for the polymerization of *rac*-LA in the presence of excess alcohol. Compared with the mononuclear counterparts, the tetra-coordinate dinuclear aluminum complexes enabled a few fold boosts in activity, but gave atactic PLAs with broadened PDIs.

## Introduction

Polylactide (PLA) is among the most important synthetic polymers, and its renewability, biodegradability and biocompatibility makes it an attracting material not only for biomedical applications, but also for using in packaging, agriculture as a commodity plastic.[1] The chain microstructure of PLA is one of the crucial factors that influence its physical, mechanical and degradable properties.[2] Isotactic poly(lactide) (*i*PLA) derived from *rac*-lactide (*rac*-LA) possesses good physical and mechanical properties when compared with the commercially available homochiral PLA, such as higher melting temperatures (205~210 °C *vs.* 170 °C of PLLA)[3] and better crystallinity.[4] To date, many efforts have been devoted to obtaining highly isotactic PLA via stereoselectively catalytic ROP of *rac*-LA.[5] However, only a few examples of adopted metal initiators proved to be isoselective, and most of them are derived from aluminum complexes.[6] Isoselective initiators based on zinc,[7] indium,[8] gallium,[9] potassium,[10] copper,[11] group 4 metals[12] and rare-earth metals[13] are still rare.

Aluminum complexes bearing chiral or achiral salen-type ligands are by far the most successful systems in generating isotactic PLA from *rac*-LA. The pioneering work of Spassky and coworkers discovered that an enantiomerically pure, chiral complex (*R*)-(SalBinap)AlOCH$_3$ was highly isoselective for the ROP of *rac*-LA ($P_m$ = 0.88).[6a] Coates' group found that a similar racemic complex *rac*-(SalBinap)Al$^i$Pr was more favorable for the isoselective ROP of *rac*-LA, producing predominantly isotactic stereoblock PLAs.[6c] Upon changing the chiral bridge from binaphthyl to biphenyl, Gibson and

[a] *Shanghai Key Laboratory of Functional Materials Chemistry and Laboratory of Organometallic Chemistry, East China University of Science and Technology, 130 Meilong Road, Shanghai 200237, People's Republic of China. Fax/Tel: +86 21 64253519; E-mail: haiyanma@ecust.edu.cn (H. Ma).*

†Electronic Supplementary Information (ESI) available: CCDC reference numbers 1063153, 1014455-1014461, 1063156 for $\mathbf{L^2H_2}$, **1**–**3**, **6** and **8**–**11**; CIF files and crystallographic data for $\mathbf{L^2H_2}$, **1**–**3**, **6** and **8**–**11**; $^1$H and $^{13}$C NMR spectra of all complexes and related NMR reactions, homonuclear decoupled $^1$H NMR spectra of typical polymer samples. See DOI: 10.1039/x0xx00000x

coworkers observed that the tacticity control in the ROP of *rac*-LA initiated by the corresponding racemic aluminum complex was partly lost, although companied by an increase of the activity.[14] Apparently, the increase of the flexibility of the chiral bridge is not favorable for the isoselectivity but is beneficial for the activity of these salen aluminum complexes toward *rac*-LA polymerization. Moreover, based on the structures of *O*-lactate model complexes, the active species of aluminum initiators bearing salen-type ligand with an achiral bridge have been well studied by Nomura's and Chen's groups (Chart 1).[15] The flexible nature of the alkanediyl bridge in these species enables a configurational inversion of the Al center after the insertion of a disfavored lactide isomer, which indicates a chain-end control mechanism. In contrast to this, although aluminum complexes with chiral salen-type ligands play a very important role in the isoselective ROP of *rac*-LA, a further study concerning the active species remains unknown. Therefore, in this work, two methyl groups were introduced at the 6,6' positions of the biphenyl bridge and the corresponding aluminum complexes were synthesized, with an aim of obtaining an optimization in both isoselectivity and activity. Meanwhile, the structures of aluminum *O*-lactate model complexes bearing salen-type ligands with a chiral bridge (6,6'-dimethyl-1,1'-biphenyl or binaphthyl) were studied in detail, in order to have a better understanding on the polymerization mechanism.

**Chart 1.** Aluminum *O*-lactate model complexes bearing achiral salen-type ligands

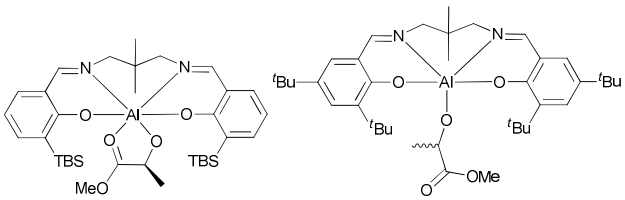


Nomura *et al*. Chen *et al*.

Dinuclear metal complexes exhibit distinctively catalytic properties toward *rac*-LA polymerization and they are relatively scarce *versus* the well-defined mononuclear analogues. In most cases, dinuclear catalysts show cooperative effect between the two metal centers, which normally leads to higher polymerization activities and even some unexpected effects.[16] In order to learn more about the catalysis of bimetallic systems, we also studied the ROP of *rac*-LA initiated by the dinuclear complexes bearing the same 6,6'dimethylbiphenyl bridged salen-type ligands.

## Results and discussion

### Synthesis and Characterization of Mono- and Dinuclear Aluminum Methyl Complexes

The reactions of racemic 6,6'-dimethylbiphenyl bridged salen-type proligands $\mathbf{L^{1-3}H_2}$ with $AlMe_3$ in a 1:1 molar ratio in toluene at 110 °C afforded the corresponding mononuclear aluminum methyl complexes **1–3** as yellow solids after recrystallization with a mixture of toluene and *n*-hexane (Scheme 1). The reaction of proligand $\mathbf{L^4H_2}$ with $AlMe_3$ via the same method mainly yielded the target complex $\mathbf{L^4}$AlMe, but further purification failed to give an analytically pure product due to its poor solubility in common organic solvents. The $^1$H NMR spectra of complexes **1–3** indicate the absence of diastereomers, despite that two stereogenic centers are involved in the structure. Notably, complex **1** with methyl groups substituted at the *ortho*-positions of phenolate rings shows fluxional behavior in solution, and broad signals accounting for the ligand framework are displayed thoroughly in the $^1$H NMR spectrum at ambient temperature. In contrast, two sets of proton resonances are displayed for the two half parts of the salen ligands of complexes **2** and **3**, indicating that they possess an asymmetric and rigid configuration in solution.

When proligands $\mathbf{L^{1-4}H_2}$ were treated with two equiv. of $AlMe_3$ in toluene at 110 °C, the desired dinuclear complexes **4–7** could be obtained (Scheme 1), as evidenced by the appearance of the methyl resonance in the upfield region (−0.48 to −0.75 ppm) and an 6:1 integral ratio of this signal to that of the two imine protons in the $^1$H NMR spectra. Complexes **4–6** could be isolated readily in high yields (70–74%) via recrystallization with a mixture of toluene and *n*-hexane; whereas complex **7** was only obtained in a very poor yield (10%) due to necessarily repeated recrystallization processes. The resonances of two methyl groups on the biphenyl moiety and the imine protons both display as one singlet in the $^1$H NMR spectra, indicative of the symmetric nature of complexes **4–7** in solution. Unexpectedly, the four Al-C$H_3$ groups of complexes **4–7** resonate as two singlets in the upfield region, suggesting the inequivalent environments of the two methyls on each aluminum center, likely arising from the restricted rotation of the biphenyl moiety.[17]

Journal Name

ARTICLE

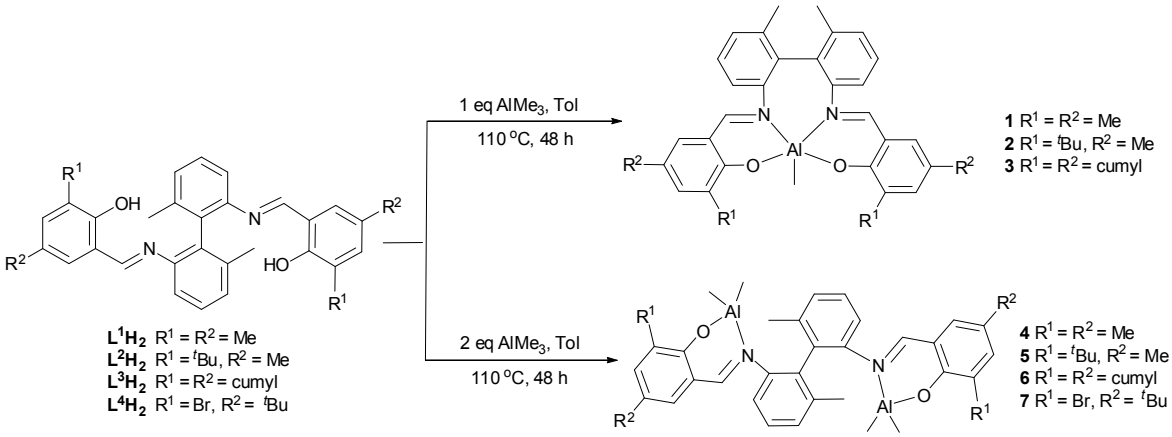


**Scheme 1** Synthesis of the mono- and dinuclear aluminum methyl complexes **1**-**7**.

Diffraction-quality crystals of complexes **1**-**3** and **6** were obtained from their saturated toluene/*n*-hexane solutions and further characterized by single-crystal X-ray diffraction studies. ORTEP views of the molecular structures of complexes **2**, **6** with selected bond lengths and angles are shown in Figs. 1 and 2. The molecular structures of complexes **1**, **3** are shown in Fig. S2, S3 (see ESI).

As shown in Fig. 1, in the solid state the aluminum center of complex **2** is five-coordinated by the tetradentate $\{ONNO\}^{2-}$ ligand and one methyl ligand. Two largest angles around the aluminum center are O2–Al1–N1 = 169.00(10)° and O1–Al1–C1 = 123.24(11)°, which give a $\tau$ value of 0.77.[18] The $\tau$ values of 0.89 and 0.82 of complexes **1**, **3** are obtained accordingly. Obviously, in these mononuclear complexes, the aluminum center adopts a distorted trigonal bipyramidal coordination geometry (tbp). In complex **2**, the two axial positions are occupied by N1 and O2, and the equatorial positions are occupied by the other three atoms. Such an orientation leads to a slightly elongated Al1–N1 bond (2.078(2) Å) relative to Al1–N2 bond (1.989(2) Å), thus a weaker interaction between the aluminum center and N1.

Moreover, complexes **1**–**3** show a $C_1$ symmetry in the solid state, and both enantiomers are found in the centrosymmetric crystal structures. As expected, an $S_a$ configuration of the 6,6'-dimethylbiphenyl moiety exclusively leads to a Δ configuration of the aluminum center, and *vice versa* $R_a$ leads to Λ. The dihedral angles of the two aromatic planes defined by biphenyl moieties in complexes **1**–**3** being 62.7°, 61.9°, 70.3° respectively, are obviously smaller than those of the free ligands (for instance, 89.4° in $\mathbf{L^2H_2}$, Fig. S1 in ESI).[19]

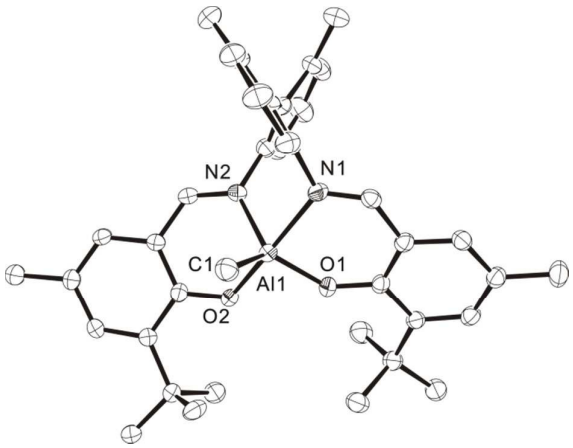


**Fig. 1** Molecular structure of **2** (all hydrogen atoms omitted for clarity; thermal ellipsoids drawn at the 50% probability level). Selected bond lengths (Å) and angles (deg): Al1–O1 1.765(2), Al1–O2 1.834(2), Al1–N1 2.078(2), Al1–N2 1.989(2), Al1–C1 1.972(3), O1–Al1–O2 89.38(9), O1–Al1–N1 87.67(9), O1–Al1–N2 122.69(10), O2–Al1–N1 169.00(10), O2–Al1–N2 87.03(9), O1–Al1–C1 123.24(11), O2–Al1–C1 96.82(11), N2–Al1–N1 85.65(9), C1–Al1–N1 93.66(11), C1–Al1–N2 113.98(11).

As depicted in Fig. 2, complex **6** shows a dinuclear feature in which both Al atoms are four-coordinate via bonding to one N donor and one O donor of the ligand as well as two methyl ligands, adopting a distorted tetrahedral geometry. The dihedral angle of the biphenyl moiety (110.7°) in complex **6** is significantly larger than those in this type of proligands (e.g. $\mathbf{L^2H_2}$, 89.4°), thus allowing sufficient separation of the two aluminum fragments. The average Al–Me bond length in complex **6** is about 1.95 Å, which is consistent with those of the other dinuclear aluminum methyl complexes.[20]

Although the coordination environments of the two aluminum centers are similar, complex **6** also shows a $C_1$ symmetry in the solid state.

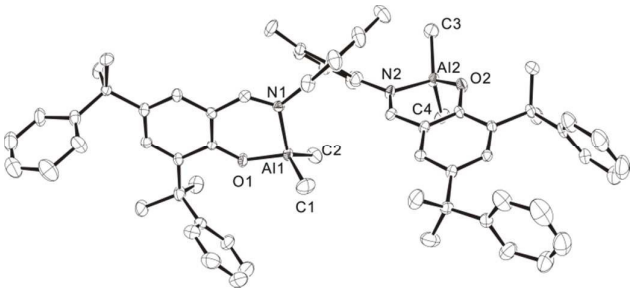


**Fig. 2** Molecular structure of **6** (all solvent molecules and hydrogen atoms omitted for clarity; thermal ellipsoids drawn at the 50% probability level). Selected bond lengths (Å) and angles (deg): Al1–O1 1.759(2), Al1–N1 1.996(3), Al1–C1 1.944(4), Al1–C2 1.939(4), Al2–O2 1.772(3), Al2–N2 1.968(3), Al2–C3 1.952(4), Al2–C4 1.956(4), O1–Al1–N1 93.55(11), O1–Al1–C1 116.21(17), O1–Al1–C2 105.12(15), C1–Al1–N1 104.57(16), C2–Al1–N1 118.22(16), C1–Al1–C2 117.19(19), O2–Al2–N2 92.93(12), O2–Al2–C3 111.64(16), O2–Al2–C4 110.38(15), C3–Al2–N2 109.51(15), C4–Al2–N2 108.40(16), C3–Al2–C4 120.44(18).

**Synthesis and Characterization of Aluminum Alkoxide Complexes**

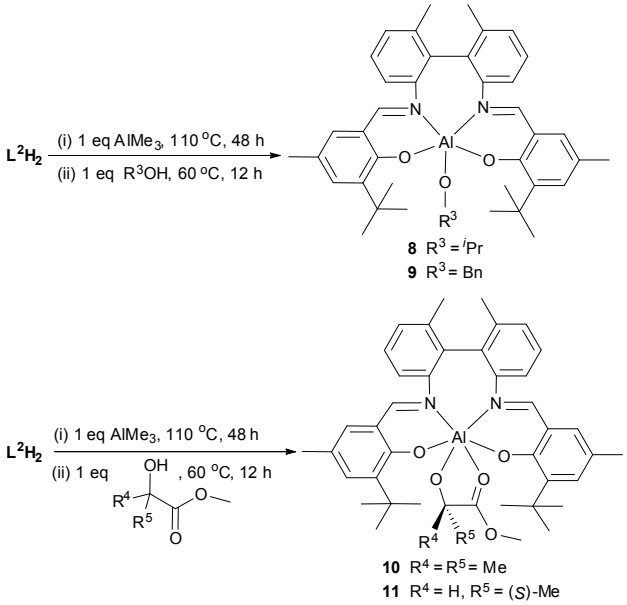


**Scheme 2** Synthesis of the alkoxide complexes **8**, **9** and *α*-alkoxy ester complexes **10**, **11**.

Due to generally better controllability and higher activities of metal alkoxide complexes toward *rac*-LA polymerization, aluminum alkoxide complexes **L**$^2$AlO$^i$Pr (**8**), **L**$^2$AlOBn (**9**) were also synthesized (Scheme 2).

The alcoholysis of the *in situ* generated complex **2** with $^i$PrOH in toluene was completed in 12 hours at 60 °C. The crude product was recrystallized readily with *n*-hexane to afford yellow crystals. The disappearance of the signal at −0.55 ppm assignable to Al–C$H_3$ protons of complex **2** and the appearance of a multiplet at 3.98 ppm attributable to the methine proton of an isopropoxy group indicate unambiguously the formation of isopropoxide complex **8**.

Notably, in the $^1$H NMR spectrum of complex **8**, the methyl resonances of the isopropyl group appear as two broad peaks with quite different chemical shifts (1.25 and 0.51 ppm), where the unusually low chemical shift of one signal is likely due to a shielding effect of neighboring aromatic rings. In the solid state (Fig. 3), complex **8** possesses a mononuclear structure with a tbp geometry, which is quite similar to that of complex **2**.

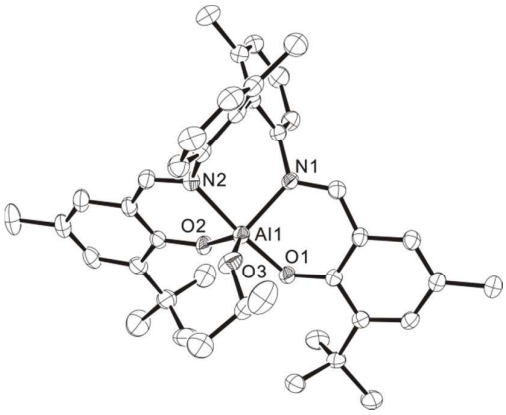


**Fig. 3** Molecular structure of **8** (all hydrogen atoms omitted for clarity; thermal ellipsoids drawn at the 50% probability level). Selected bond lengths (Å) and angles (deg): Al1–O1 1.8253(14), Al1–O2 1.7692(14), Al1–O3 1.7164(15), Al1–N1 1.9790(17), Al1–N2 2.0646(17), O1–Al1–O2 91.16(6), O1–Al1–O3 100.56(7), O2–Al1–O3 122.04(8), O1–Al1–N1 88.19(6), O2–Al1–N1 119.86(7), O3–Al1–N1 117.09(8), O1–Al1–N2 173.80(7), O2–Al1–N2 88.54(6), O3–Al1–N2 84.81(7), N1–Al1–N2 86.59(7).

A similar reaction of the *in situ* generated complex **2** with benzyl alcohol gave the corresponding complex **L**$^2$AlOBn (**9**) as yellow crystals after recrystallization with toluene (Scheme 2). The C$H_2$ protons on the benzyloxy group display as a broad signal at 4.81–4.65 ppm in the $^1$H NMR spectrum, indicative of a relatively free rotation of Al–O (Bz) bond. As shown in Fig. S4 (see ESI), complex **9** also possesses a mononuclear structure in the solid state. Interestingly, the two enantiomers of complex **9** crystallize separately. The $\tau$ value of complex **9** (0.96) is larger than that of complex **8** (0.86) and suggests almost a perfect tbp geometry around the aluminum center in complex **9**.

**Synthesis and Characterization of Aluminum *α*-Alkoxy Ester Complexes**

To gain a better understanding on the structures of active species generated in the polymerization of lactides, the isobutyrate complex **L**$^2$Al(OCMe$_2$CO$_2$Me) (**10**) and *O*-lactate complex **L**$^2$Al[(*S*)-OCHMeCO$_2$Me] (**11**) were synthesized via *in situ* alcoholysis of the parent aluminum methyl complex **2** with the corresponding *α*-hydroxy esters (Scheme 2). Noticeably, complex **11** mimics the product of the first insertion of an *L*-LA monomer.[21]

Complex **10** was recrystallized with a mixture of toluene and *n*-hexane. As illustrated in Fig. 4, two pairs of enantiomers are found in the unit cell of complex **10**, which can be denoted as Δ-$R_a$, Λ-$R_a$, Δ-$S_a$ and Λ-$S_a$. Ortep views of two typical isomers are further shown in Fig. 5 (denoted as isomers **10a** and **10b**). In all isomers, the aluminum center is six-coordinated by the tetradentate ligand and

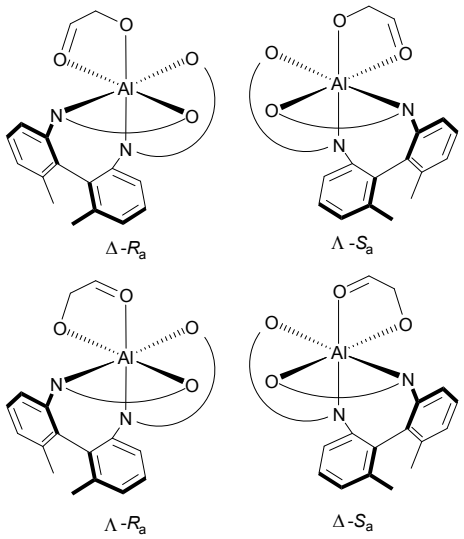


**Fig. 4** Isomers of complex **10** in the unit cell.

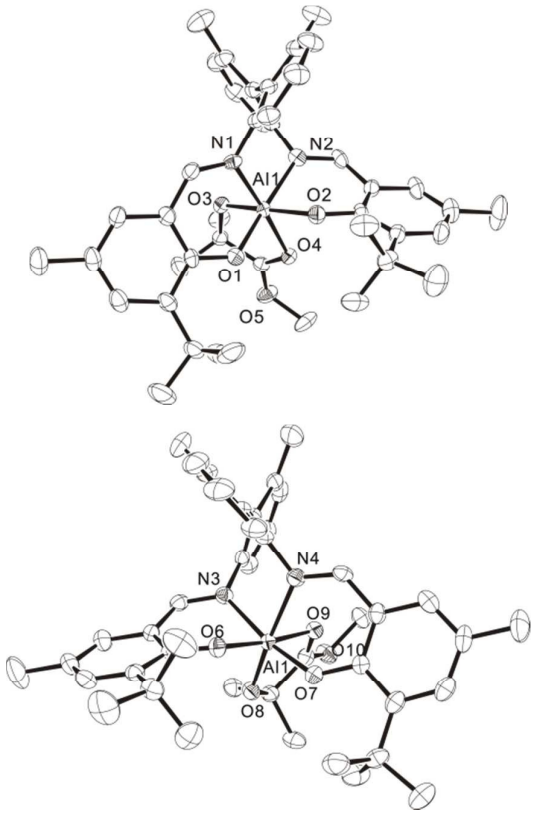


**Fig. 5** Molecular structures of **10a** (top) and **10b** (bottom) (all hydrogen atoms omitted for clarity; thermal ellipsoids drawn at the 50% probability level). Selected bond lengths (Å) and angles (deg): Al1–O1 1.847(2), Al1–O2 1.8291(19), Al1–O3 1.817(2), Al1–O4 2.0296(19), Al1–N1 2.007(2), Al1–N2 2.073(2), Al2–O8 1.8056(19), Al2–O9 2.023(2), O4–Al1–N1 175.93(9), O2–Al1–O4 88.70(8), O3–Al1–O4 82.35(8), O2–Al1–N1 94.90(9), O3–Al1–N1 94.33(9), O6–Al2–O9 171.56(9).

the $\kappa^2$-$\alpha$-alkoxy ester ligand. In isomer **10a** (Λ-$R_a$), the axial positions are occupied by the carbonyl oxygen and one nitrogen donor of the salen ligand (O4–Al1–N1 = 175.93(9)°), while in isomer **10b** (Λ-$S_a$), the axial positions are occupied by the carbonyl oxygen and one oxygen donor of the salen ligand (O6–Al2–O9 = 171.56(9)°). The Al–O (carbonyl) bond lengths (2.0296(19) Å (**10a**), 2.023(2) Å, (**10b**)) are similar, but shorter than that observed in the salen aluminum complex shown in Chart 1 reported by Nomura's group (Al–O (carbonyl) = 2.165 Å).[15a]

Surprisingly, only one set of peaks are displayed in the $^1$H NMR spectrum of complex **10** and no resonances belonging to another pair of enantiomers could be detected. The two half fragments of the tetradentate ligand are still asymmetric, showing resonances similar to that of complex **2** but more separated from one another. On account of the inherent axial chirality of the $\{ONNO\}^{2-}$ ligand, an epimerization of the chiral metal center in complex **10** in solution probably due to a fast configuration interconversion is therefore assumed. To verify this hypothesis, variable temperature $^1$H NMR spectra of complex **10** were determined in toluene-$d_8$ in the temperature range of −40 °C to 80 °C (Fig. S27 in ESI). However, except for slight shifts of some signals with the variation of temperature and certain broadening of all signals observed at 80 °C, no extra peaks appear and the asymmetric pattern of the tetradentate ligand is retained within the entire temperature range. These features to a great extent exclude the suspicion of the fluxional behavior of the chiral 6,6'-dimethylbiphenyl bridge,[22] and further indicates that the epimerization of the chiral metal center in solution is more likely due to a dynamic process involving the $\alpha$-alkoxy ester ligand. Nevertheless, a significant downfield shift of the carbonyl resonance (193.6 ppm) in the $^{13}$C NMR spectrum of complex **10** is observed when compared to that of methyl isobutyrate (176.1 ppm), which normally suggests a stable coordination of the carbonyl to the metal center. Thereby, it seems that we are in a conflict situation.

We then turned to $^{27}$Al NMR spectroscopy to get some insight into the coordination environment of the aluminum center in complex **10**. For a comparison purpose, the $^{27}$Al NMR spectra of the mononuclear aluminum complex **2** and the dinuclear complex **5** were also determined. Surprisingly, two different resonances are observed in the $^{27}$Al NMR spectrum of complex **10** (Fig. S28B in ESI), with one broad peak at about 70 ppm ($w_{1/2}$ = 2657 Hz) and a shoulder at about 25–39 ppm; while only one broad peak at about 72-74 ppm is observed in the $^{27}$Al NMR spectra of complexes **2** and **5** (Fig. S28A in ESI). It is generally accepted that for aluminum complexes bearing with salen-type ligands, four-coordinate aluminum center has a chemical shift centered at ~70 ppm, five-coordinate at ~40 ppm and six-coordinate at ~0 ppm.[6e,6f,15b,23] For instance, Feijen's group reported that the aluminum isopropoxide complex with a *rac*-cyclohexylsalen ligand displays a single resonance at 35.45 ppm, in line with a five-coordinate aluminum center.[6e] Duda and coworkers proposed a four-coordinate Al center of the living lactide oligomer derived from the (SalBinap)Al$O^i$Pr complex for displaying a single Al resonance at 67 ppm.[6f] Tolman's group also reported a series of five-coordinated salen aluminum complexes with Al resonances at about 35 ppm.[23c] Thus, by taking into consideration the $^{27}$Al NMR data of the dinuclear complex **5** and the related salen aluminum complexes reported in literatures,[6e,6f,15b,23] it is conceivable that for complex **10** the main Al resonance at about 70 ppm could be attributed to a four-coordinate aluminum center, while the shoulder at 25–39 ppm to a five-coordinate aluminum center. Moreover, the Al resonance at ~74

ppm of complex **2** further reals the dissociation of one nitrogen donor of the {ONNO}$^{2-}$ ligand in solution, likely the one occupying the axial position of the trigonal bipyramid (having a weaker interaction with Al center), although a five-coordinate metal center of complex **2** is found in the solid state. In Duda's work, the dissociation of two nitrogen donors of the SalBinap ligand was even proposed to account for the four-coordinate aluminum center of the living lactide oligomer.[6f] Based on these results, the four-coordinate aluminum center of complex **10** could be constructed either by a $\kappa^3$-{ONNO}$^{2-}$ ligand and a $\kappa^1$-$\alpha$-alkoxy ester ligand, or by a $\kappa^2$-{ONNO}$^{2-}$ ligand and a $\kappa^2$-$\alpha$-alkoxy ester ligand. In the latter case, in combination with the inherent axial chirality of the salen ligand, the $\kappa^2$-chelating mode of the $\alpha$-alkoxy ester ligand would lead to the generation of diastereomers, which however are not observed in our work. Therefore, we suggest that in the four-coordinate structure the chiral salen ligand is tridentately coordinated and the $\alpha$-alkoxy ester group acts as a monodentate ligand.

A comparison of the hydrodynamic radius of complex **10** ($r_H$ = 6.03 Å) determined by DOSY experiments with the X-ray radius estimated from its solid-state structure ($r_{X\text{-}ray}$= 6.90 Å) suggests that the complex should be monomeric in solution.[24] Thus, the five-coordinate metal center detected in the $^{27}$Al NMR spectrum of complex **10** is unlikely resulted from any aggregation of aluminum species, but most likely a coordination of the carbonyl group of the $\alpha$-alkoxy ester ligand instead based on the corresponding $^{13}$C NMR data. The coexistence of both four- and five-coordinate aluminum centers of complex **10** in solution indicates the dynamic coordination of this group. The hemilabile coordination mode of the carbonyl group in an $\alpha$-alkoxy ester has also been reported in literatures. As shown in Chart 1, by varying the substituents on the phenolate rings, the coordination mode of the carbonyl group of the $\alpha$-alkoxy ester ligand is different.[15] Our group also reported some zinc *O*-lactate complexes bearing chiral aminophenolate ligands, where a hemilabile chelating interaction of the carbonyl group has been observed in single crystal cell unit, as indicated by quite different distances of zinc to carbonyl oxygen (2.525(4) Å vs. 2.212(4) Å).[25] Although the $^{13}$C NMR spectrum of complex **10** suggests the stable coordination of carbonyl group to aluminum, the $^{27}$Al NMR data do indicate an equilibrium between dissociation and association states of the carbonyl group, which also explain well the "disappearance" of diastereomers in solution as characterized by $^1$H and $^{13}$C NMR spectroscopy. The disagreement among different NMR spectroscopy is likely due to the different NMR time scales adopted in the measurement.

Similar structure features are also found for complex **11**. As depicted in Fig. 6, in the solid state the aluminum center of **11** is six-coordinated by the tetradentate {ONNO}$^{2-}$ ligand and two oxygen atoms from (*S*)-lactate. Four isomers are found in the unit cell, which can be denoted as Δ-$S_aS$, Λ-$S_aS$, Λ-$R_aS$ and Δ-$R_aS$ due to the existence of an extra stereogenic center from (*S*)-lactate. The Al–O (carbonyl) bond lengths (2.039(2) Å (**11a**), 2.0238(2) (**11b**)) are slightly longer than those of complex **10**. Again, despite of the presence of three stereogenic centers, only a pair of diastereomers in a 1:1 molar ratio is observed in solution via $^1$H NMR spectroscopy. For instance, two peaks accounting for the methine proton of the lactate fragment are displayed at 4.48 and 4.29 ppm, and the methoxy group also shows two resonances at 3.06 and 2.90 ppm. In the $^{13}$C NMR spectrum of complex **11**, resonances of the carbonyl group appear at 189.8 and 189.0 ppm, which further indicate the coordination state of the carbonyl group. Similarly, two different Al resonances at about 69 and 25–41 ppm are observed in the $^{27}$Al NMR spectrum of complex **11**. Therefore, a fast equilibrium between four- and five-coordinate metal centers arising from the dissociation and association of the carbonyl group is also suggested for complex **11** in solution.

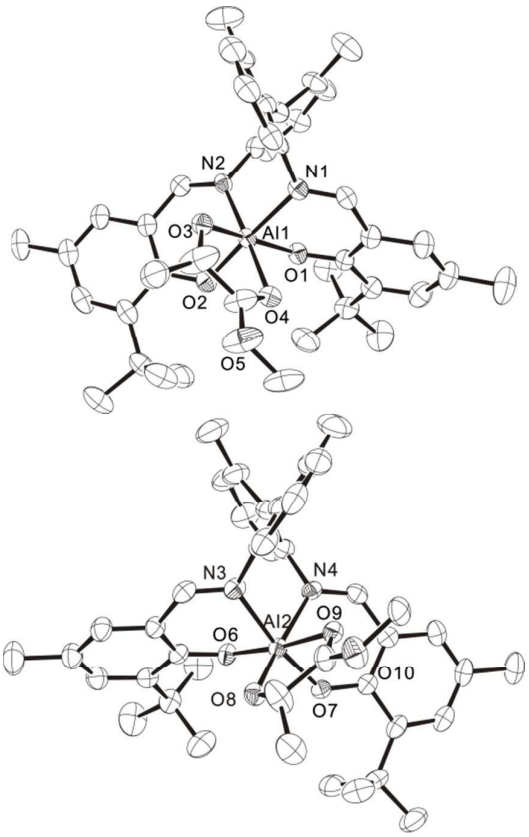


**Fig. 6** Molecular structures of **11a** (top) and **11b** (bottom) (all hydrogen atoms omitted for clarity; thermal ellipsoids drawn at the 50% probability level). Selected bond lengths (Å) and angles (deg): Al1–O1 1.822(2), Al1–O2 1.849(2), Al1–O3 1.812(2), Al1–O4 2.039(2), Al1–N1 2.063(3), Al1–N2 2.005(3), Al2–O8 1.808(2), Al2–O9 2.038(2), O4–Al1–N2 176.94(10), O1–Al1–O2 91.47(10), O2–Al1–O3 95.16(10), O1–Al1–N1 85.33(10), O3–Al1–N1 87.99(10), O6–Al2–O9 172.33(10).

**Ring-Opening Polymerization of *rac*-LA by Complexes 1–3, 8–11**

Mononuclear complexes **1–3** and **8–11** could effectively initiate the ROP of *rac*-LA, producing PLAs with narrow PDIs. The main results of the polymerization studies are summarized in Table 1. Complex **1** with *ortho*-methyl groups on the phenolate rings displayed the highest catalytic activity among three mononuclear aluminum methyl complexes. In the absence of alcohol, the polymerization went to 96% monomer conversion within 72 h at 110 °C in toluene (Table 1, entry 1). Complex **2** proved to be much less active than complex **1** (Table 1, entry 3), and a monomer conversion of 78% was reached after 132 h; whereas complex **3** bearing *ortho*-cumyl groups proved to be relatively more active than complex **2** (92% after 132 h, Table 1, entry 5). In general, the ROP of *rac*-LA initiated

by these mononuclear aluminum methyl complexes gave broadly distributed polymers ($M_w/M_n$ = 1.40–2.06) with molecular weights higher than the calculated values, indicating an insufficient initiation. The resultant PLAs are isotactic-enriched with $P_m$ values between 0.66 and 0.60. A decreasing tendency of the isoselectivity with the increase of the steric bulkiness of the *ortho*-substituents on the phenolate rings could be observed for complexes **1–3**, which is similar to Gibson's result.[14] Unfortunately, the introduction of two methyl groups at the 6,6'-positions of the biphenyl bridge has little influence on the isoselectivity when compared with the bald biphenyl bridged salen aluminum complexes.[14]

In order to acquire better initiation efficiencies and well-controlled polymerization procedures, *rac*-LA polymerizations were initiated by aluminum isopropoxides generated *in situ* via strictly controlling the molar ratio of complexes **1–3** and $^{i}$PrOH. The polymerizations were much faster when compared with those without $^{i}$PrOH (Table 1, entries 2, 4 and 6). For example, a monomer conversion of 96% could be achieved by complex **1** within 72 h, while the addition of $^{i}$PrOH significantly shortened the polymerization time to 24 h to reach a similar conversion of 92% (Table 1, entries 1 and 2). All the resultant polymers are isotactic enriched ($P_m$ = 0.65–0.73) and possess very narrow molecular weight distributions (PDI = 1.03–1.05). For the catalytic system **2**/$^{i}$PrOH, a linear relationship of $M_n$ of the PLA samples *versus* monomer conversion is observed (Fig. S35 in ESI). Meanwhile, the polydispersity indices are ranging from 1.03 to 1.06, suggesting "living" characters of the polymerization process.

In spite of the different initiating groups, polymerization behaviors of complexes **8–11** are similar. High monomer conversions around 85% could be reached within 80–96 h. A slight increase in the isotacticity of the resultant polymers is also observed ($P_m$ = 0.65–0.68) when compared with those obtained by complex **2** with or without $^{i}$PrOH.

For a purpose of investigating the exact influence of ligand substituents on the polymerization rate of *rac*-LA, polymerization kinetics was systematically investigated with complexes **1–3** in the presence of $^{i}$PrOH by adopting an initiator/$^{i}$PrOH/monomer ratio of 1:1:100 ([*rac*-LA]$_0$ = 1.0 mol/L) at 110 °C in toluene. The semilogarithmic plots for these polymerizations are shown in Fig. S36 (see ESI). To our surprise, curved lines consisting of two linear stages are obtained for complexes **1** and **2**; while a simply linear relationship is obtained for complex **3** thoroughly. Such a two-stage-kinetics has previously been reported by Okuda's group for the ROP of *L*-LA initiated by rare earth metal silylamido complexes,[26] but it is quite unusual for aluminum initiators. In the case of complex **1**, the $k_{app}$ value of the first stage is (18.9 ± 1.5) × $10^{-2}$ $h^{-1}$, which is more than two times higher than that of the second stage ((8.60 ± 0.39) × $10^{-2}$ $h^{-1}$). Moreover, the turn point appears at a monomer conversion of ca. 50%. As for complex **2**, the turn point emerges earlier when a monomer conversion of 30% is just reached. Taking all these features into consideration, it seems that the first stage becomes shorter with the increase of the steric bulkiness of the aluminum complexes. Therefore, it is suspected that such a two-stage-kinetics might be resulted from some bimolecular processes or aggregations of aluminum species. To verify this suspicion, kinetics of *rac*-LA polymerization initiated by well-defined isopropoxide complex **8** was systematically investigated at various initiator concentrations (0.01, 0.008, 0.0067 and 0.0057 mol/L) with respect to a constant monomer concentration ([*rac*-LA]$_0$ = 1.0 mol/L). Due to very low monomer conversions, the first stage of each polymerization run could not be clearly presented. However, from the intercepts at Y axis, it is obvious that, with the decrease of initiator concentration, the first fast-polymerization stage becomes shorter and tends to vanish (Fig. S37A in ESI). By plotting ln $k_{app}$ *versus* ln [**8**], a linear line with a slope of 1.13 was obtained for the second stage of polymerization (Fig. S37B in ESI), indicating first-order kinetics in both monomer and initiator concentrations, thus the monomeric nature of the aluminum active species in the second stage. Based on these results, it is reasonable to suggest that, some extent of aggregation or coorperation of aluminum species might occur in the earlier stage of *rac*-LA polymerization when a less sterically hindered initiator is adopted and meanwhile the initiator concentration is also relatively high.[27] Since different active species are suggested to be involved in

**Table 1** ROP of *rac*-LA initiated by complexes **1–3**, **8–11**.[a]

| Entry | Cat. | [LA]$_0$/[Cat.]$_0$/[$^{i}$PrOH]$_0$ | Time (h) | Conv.[b] (%) | $M_{n,cacld}$[c] (× $10^4$) | $M_n$[d] (× $10^4$) | PDI[d] | $P_m$[e] | $k_{app}$ (×$10^{-2}$ $h^{-1}$) |
|---|---|---|---|---|---|---|---|---|---|
| 1 | **1** | 100:1:0 | 72 | 96 | 1.38 | 3.09 | 2.06 | 0.66 | |
| 2 | **1** | 100:1:1 | 24 | 92 | 1.33 | 1.62 | 1.05 | 0.73 | 8.60 ± 0.39 |
| 3 | **2** | 100:1:0 | 132 | 78 | 1.12 | 1.17 | 1.48 | 0.63 | |
| 4 | **2** | 100:1:1 | 120 | 91 | 1.31 | 1.68 | 1.04 | 0.65 | 1.89 ± 0.11 |
| 5 | **3** | 100:1:0 | 132 | 92 | 1.33 | 1.56 | 1.40 | 0.60 | |
| 6 | **3** | 100:1:1 | 60 | 90 | 1.30 | 1.46 | 1.03 | 0.65 | 3.94 ± 0.18 |
| 7 | **8** | 100:1:0 | 96 | 86 | 1.24[f] | 1.39 | 1.05 | 0.68 | 1.98 ± 0.03 |
| 8 | **8** | 100:1:1 | 81 | 85 | 0.61[f] | 0.69 | 1.06 | 0.66 | 2.13 ± 0.07 |
| 9 | **8** | 100:1:2 | 64 | 83 | 0.40[f] | 0.46 | 1.06 | 0.68 | 2.73 ± 0.02 |
| 10 | **8** | 100:1:3 | 88 | 92 | 0.33[f] | 0.35 | 1.08 | 0.66 | 2.91 ± 0.04 |
| 11 | **9** | 100:1:0 | 78 | 84 | 1.21 | 1.42 | 1.06 | 0.68 | 2.21 ± 0.12 |
| 12 | **10** | 100:1:0 | 81 | 84 | 1.21 | 1.70 | 1.04 | 0.65 | 2.17 ± 0.15 |
| 13 | **11** | 100:1:0 | 83 | 86 | 1.24 | 1.45 | 1.05 | 0.66 | 2.21 ± 0.06 |

[a] [*rac*-LA]$_0$ = 1.0 M, toluene, 110 °C; [b] Determined by $^1$H NMR spectroscopy; [c] $M_{n,cacld}$ = ([*rac*-LA]$_0$/[cat.]$_0$) × 144.14 × Conv.%; [d] Determined by GPC with polystyrenes as standards; [e] $P_m$ is probability of forming a new m-dyad, determined by homonuclear decoupled $^1$H NMR spectroscopy; [f] $M_{n,cacld}$ = {[*rac*-LA]$_0$/([$^{i}$PrOH]$_0$ +[cat.])} × 144.14 × Conv.%.

different polymerization stages, a variation of stereoselectivity is more or less expected. However, it is found that the polymers obtained at different polymerization stages possess almost the same tacticity. Probably, the aggregation or coorperation of aluminum species may have little influence on the selectivity, or most likely the difference of the stereoselectivities is not remarkable on the basis of the inherently moderate isotacticity of these complexes.

Immortal polymerization provides a convenient approach for efficiently preparing PLAs with various molecular weights,[28] thus the reaction of complex **8** with as high as 50 equiv. of $^{i}$PrOH was monitored by $^{1}$H NMR spectroscopy. In the spectrum, no signals attributable to the free salen ligand are observed (Fig. S29 in ESI). A set of resonances could be assigned to the salen ligand moiety, but are obviously different from those of complex **8**. Except for the strong resonances at 3.86, 3.45 and 1.09 ppm assignable to $^{i}$PrOH, no other signals accounting for the isopropoxyl group of a metal complex could be found. All these indicate that in the presence of excess isopropanol the unexpected ligand dissociation does not occur and a fast exchange between Al-O$^{i}$Pr and free $^{i}$PrOH takes place instead. The ROP of *rac*-LA was then promoted by complex **8** at 110 $^{o}$C upon adding an excess of $^{i}$PrOH as a chain transfer agent. The immortal polymerization was evidenced by the small PDI values (1.06–1.08) as well as a good agreement between the observed $M_n$ values and the calculated ones (Table 1, entries 8, 9 and 10).[29] Due to the low activities of these series of mononuclear complexes, *rac*-LA polymerizations in both high monomer and alcohol loadings are not further investigated.

The $^{1}$H NMR spectrum of a purified *rac*-LA oligomer obtained by complex **8** clearly shows the existence of both terminal groups of $(CH_3)_2CHO$– and $HOCH(CH_3)CO$–, according to the resonances at about 1.22, 4.95 ppm for the former and 1.48, 4.37 ppm for the latter (Fig. S38 in ESI). Moreover, a series of peaks end-capped with an isopropoxy and a hydroxyl group dominate in the ESI-TOF mass spectrum (Fig. S39 in ESI), indicating an initiation via Al–O$^{i}$Pr bonding as well as a coordination-insertion polymerization.[30]

To get more insight into the mechanism of stereoselective *rac*-LA polymerization initiated by these racemic salen aluminum complexes, the tetrad signals of a typical PLA sample obtained by complex **1** (Table 1, entry 2) was analyzed via homonuclear decoupled $^{1}$H NMR spectroscopy. As depicted in Fig. S40 (see in ESI), the integrals of *sis*, *sii*, *iis*, and *isi* tetrad peaks give an approximate ratio of 1:1.7:1.5:1.6. The relatively small *sis* signal and a close intensity ratio of *sii* : *iis* : *isi* to 1:1:1 suggest that the polymer main chain is stereoblock-enriched.[6c,7a] Coates and coworkers reported that the formation of stereoblock PLAs via *rac*-LA polymerization initiated by *rac*-(SalBinap)AlO$^{i}$Pr is resulted from a combination of enantiomorphic site control and polymer exchange mechanisms.[6c] Accordingly, a similar polymerization procedure proceeded via a polymer exchange process between two enantiomeric active centers is suggested to be involved in the polymerization initiated by these chiral salen aluminum complexes.[31]

**Table 2** ROP of *rac*-LA initiated by complexes **4-7**.[a]

| Entry | Cat. | $[LA]_0/[Cat.]_0$ | Time (h) | Conv.[b] (%) | $M_{n,cacld}$[c] (×10$^4$) | $M_n$[d] (×10$^4$) | PDI[d] | $P_m$[e] |
|---|---|---|---|---|---|---|---|---|
| 1 | **4** | 100:1 | 10 | 90 | 0.65 | 2.46 | 1.19 | 0.56 |
| 2 | **4** | 200:1 | 22 | 92 | 1.33 | 3.73 | 1.26 | 0.56 |
| 3 | **5** | 100:1 | 14 | 90 | 0.65 | 2.59 | 1.27 | 0.54 |
| 4 | **5** | 200:1 | 24 | 87 | 1.25 | 4.34 | 1.23 | 0.53 |
| 5 | **6** | 100:1 | 16 | 89 | 0.64 | 2.34 | 1.22 | 0.50 |
| 6 | **6** | 200:1 | 24 | 85 | 1.23 | 4.24 | 1.25 | 0.50 |
| 7 | **7** | 100:1 | 24 | 67 | 0.49 | 1.97 | 1.16 | 0.49 |

[a] $[rac\text{-}LA]_0$ = 1.0 M, toluene, 110 °C; [b] Determined by $^{1}$H NMR spectroscopy; [c] $M_{n,cacld} = ([rac\text{-}LA]_0/[Al]_0) \times 144.14 \times$ Conv.%; [d] Determined by GPC with polystyrenes as standards; [e] $P_m$ is probability of forming a new m-dyad, determined by homonuclear decoupled $^{1}$H NMR spectroscopy.

Since the isoselectivity of these series of aluminum complexes toward *rac*-LA polymerization is partly lost when compared to the one bearing a binaphthyl-bridged salen ligand, the *α*-alkoxy ester model complex *rac*-(SalBinap)Al($OCMe_2CO_2Me$) was prepared on an NMR scale and characterized spectroscopically, with an attempt to find some structural difference between these two systems. The NMR scale reaction of *rac*-(SalBinap)AlMe with methyl 2-hydroxyisobutyrate afforded the target *α*-alkoxy ester complex. Only one set of peaks in the $^{1}$H and $^{13}$C NMR spectra (Fig. S30 and S31 in ESI) as well as two peaks at about 70 and 34 ppm in the $^{27}$Al NMR spectrum are observed (Fig. S32 in ESI), which suggest the same coordination patterns of the salen and *α*-alkoxy ester ligands in *rac*-(SalBinap)Al($OCMe_2CO_2Me$) as those in complex **10**. Therefore, the structural features of these two systems are basically the same; the poor isoselectivity of the chiral aluminum complexes reported in this work is likely caused by the less sterically hindered 6,6'-dimethylbiphenyl bridge, rather than the dissociation of one N donor of the ligand and an equilibrium between the association and dissociation states of the carbonyl group in the active species.

As mentioned above, although the rigid chiral bridge in these complexes results in a dissociation of one N donor of the chiral salen ligand in solution, unlike the achiral ones, the chiral salen ligand moiety in these aluminum complexes shows no fluxional behavior in a broad temperature range, which is then suggested to be the original of an enantiomorphic site control.

### Ring-Opening Polymerization of *rac*-LA by Complexes 4–7

The dinuclear aluminum complexes **4–6** could enable 3–6 fold boosts in activity toward *rac*-LA polymerization in comparison with their mononuclear aluminum counterparts,[16] but lead to atactic PLAs ($P_m$ = 0.50–0.56) (Table 2). For instance, monomer conversions of nearly 90% could be reached within 10 to 16 h at a $[rac\text{-}LA]_0/[initiator]_0$ ratio of 100, and within 22 to 24 h at a ratio of 200 (Table 2, entries 1 to 6). Among them, complex **4** with *ortho*-methyl

groups on the phenolate rings displays the highest catalytic activity (Table 2, entry 1). The introduction of electron-withdrawing bromo-substituents in complex **7** leads to a much lower activity, with a conversion of 67% reached only within 24 h at a [*rac*-LA]$_0$/[initiator]$_0$ ratio of 100 (Table 2, entry 7).

As shown in Table 2, the experimental molecular weights of resultant PLAs are much higher than the theoretical values, obviously due to an insufficient initiation of aluminum methyl complexes. Thereby, the end-groups of typical *rac*-LA oligomer were analyzed via $^1$H NMR spectroscopy and MALDI-TOF mass spectrum. However, both methods gave no conclusion on the initiating group (Fig. S41 in ESI). In attempts to generate *in situ* the corresponding metal-alkoxide species, we found that the treatment of typical dinucear complex **6** with one equiv. of alcohols such as $^i$PrOH, BnOH and $^t$BuOH all led to partial dissociation of the salen ligand, even in the presence of the *rac*-LA (Fig. S33 and S34 in ESI). Thus, it seems that these series of dinuclear aluminum complexes are quite sensitive toward proton sources. Most likely, during the polymerization process the active species were generated by reacting with impurities (brought with the monomers, e.g. lactic acid, hydrolyzed lactide, water)[32] via the cleavage of Al–O$_{aryl}$ as well as Al–Me bonds. This explains well the unusually low activity of complex **7**. With electron-withdrawing groups on the phenolate rings, all these bonds become stronger, therefore less reactive, resulting in slow initiation efficiency.

## Conclusions

A series of mononuclear aluminum complexes [**L$^{1-3}$**AlMe] (**1**–**3**), dinuclear aluminum complexes [(**L$^{1-4}$**)$_2$Al$_2$Me$_4$] (**4**–**7**), well-defined alkoxide complexes **L$^2$**Al$O^i$Pr (**8**), **L$^2$**AlOBn (**9**) and *α*-alkoxy ester complexes **L$^2$**Al(OCMe$_2$CO$_2$Me) (**10**), **L$^2$**Al[(*S*)-OCHMeCO$_2$Me] (**11**) have been synthesized and fully characterized. X-ray diffraction studies of typical aluminum complexes revealed that, in the solid state the mononuclear aluminum methyl and alkoxide complexes all possess a five-coordinate metal center with a distorted trigonal bipyramidal geometry (tbp); while the dinuclear complexes possess four-coordinate aluminum centers adopting distorted tetrahedral geometries. Complexes **10** and **11** are the first examples of aluminum *α*-alkoxy ester complexes bearing a chiral bridged salen ligand, and their solid structures reveal that the aluminum center is six-coordinated with the tetradentate ligand and the *α*-alkoxy ester ligand that chelates onto the Al center in a $\kappa^2$-O (alkoxide), O (carbonyl) fashion. The presence of two Al resonances in the $^{27}$Al NMR spectra of complexes **10** and **11** suggests an exchange process between four- and five-coordinate aluminum species in solution, which is likely resulted from an association/dissociation equilibrium of the carbonyl group of the *α*-alkoxy ester ligand. All of these aluminum complexes exhibit moderate catalytic activity toward the ROP of *rac*-LA. The polymerization initiated by **1**–**3**/$^i$PrOH shows living features, affording isotactic enriched PLAs ($P_m$ = 0.65–0.73) with narrow molecular weight distributions. Detailed kinetic studies suggested that some extent of aggregation or coorperation of aluminum species might occur in the earlier stage of *rac*-LA polymerization when a less sterically hindered initiator such as complex **1** or **2** is adopted and meanwhile the initiator concentration is relatively high. Complexes **8–11** showed similar performances as the **2**/$^i$PrOH catalytic system, and in the presence of excess isopropanol the polymerization initiated by complex **8** could even take place in an immortal manner. Owing to less hindered metal centers and undesired dissociation reactions, the dinuclear aluminum complexes only afforded atactic PLAs, but resulted in 3–6 fold boosts in activity.

## Experimental Section

### General considerations

All manipulations were carried out under a dry argon atmosphere using standard Schlenk-line or glovebox techniques. Toluene and *n*-hexane were refluxed over sodium benzophenone ketyl prior to use. Benzene-$d_6$, toluene-$d_8$, chloroform-$d$, and other reagents were carefully dried and stored in a glovebox. Proligand **L$^{1-3}$H$_2$** were synthesized according to literature methods.[33] *rac*-LA (Aldrich) was recrystallized with dry toluene and then sublimed twice under vacuum at 80 °C. $^i$PrOH was dried over calcium hydride prior to distillation. All other chemicals were commercially available and used after appropriate purification. 25 mL Schlenk tube used in the polymerization were dried under vacuum with gas flame, and exposed to a vacuum-argon cycle three times.

NMR spectra were recorded on Bruker AVANCE spectrometers at 25 °C ($^1$H, 400 MHz; $^{13}$C, 100 MHz; $^{27}$Al, 130.3 MHz) unless otherwise stated. Chemical shifts for $^1$H and $^{13}$C NMR spectrum were referenced internally using the residual solvent resonances and reported relative to tetramethylsilane. $^{27}$Al chemical shifts were referenced to an external 1.1 M solution of Al(NO$_3$)$_3$ in D$_2$O. Elemental analyses were performed on an EA-1106 instrument. Spectroscopic analyses of polymers were performed in CDCl$_3$. Gel permeation chromatography (GPC) analyses were carried out on an Agilent instrument (L1200 pump, Optilab Rex injector) in THF at 35 °C at a flow rate of 1 mL/min. Calibration standards were commercially available narrowly distributed linear polystyrene samples that cover a broad range of molar masses ($10^3 < M_n < 7 \times 10^5$ g/mol). The $M_n$ values were reported without correction.

### Synthesis of proligands and aluminum complexes

**{ONNO$^{tBu,\ Br}$}H$_2$ (L$^4$H$_2$).** A 100 mL round bottom flask with magnetic stirrer bar was charged with 3-bromo-5-*tert*-butyl-2-hydroxybenzaldehyde (1.60 g, 6.23 mmol), 2,2'-diamino-6,6'-dimethyl-1,1'-biphenyl (0.69 g, 3.10 mmol) and 30 mL of ethanol. Then the mixture was refluxed for 16 h and an orange precipitate was formed during the reaction. The orange solid was isolated by filtration, washed with cold ethanol and then dried under vacuum (1.35 g, 63%). $^1$H NMR (CDCl$_3$, 400 MHz, 298 K): δ 12.74 (s, 2H, ArO*H*), 8.45 (s, 2H, N=C*H*), 7.54 (d, 2H, *J* = 2.2 Hz, Ar*H*), 7.37 (t, 2H, *J* = 7.6 Hz, Ar*H*), 7.27 (d, 2H, *J* = 7.6 Hz, Ar*H*), 7.22 (d, 2H, *J* = 2.2 Hz, Ar*H*), 6.09 (d, 2H, *J* = 7.6 Hz, Ar*H*), 2.08 (s, 6H, ArC*H*$_3$), 1.25 (s, 18H, C(C*H*$_3$)$_3$). $^{13}$C NMR (CDCl$_3$, 100 MHz, 298 K): δ 161.7 (Ar*C*=N), 155.4 (Ar*C*OH), 146.5, 142.7, 137.3, 133.6, 133.4, 129.2, 128.9, 128.2, 119.5, 115.8, 110.5 (all Ar*C*), 34.2 (*C*(CH$_3$)$_3$), 31.4 (C(*C*H$_3$)$_3$), 20.0 (Ar*C*H$_3$). Anal. Calcd. for: C$_{36}$H$_{38}$O$_2$N$_2$Br$_2$: C, 62.62; H, 5.55; N,4.06. Found: C, 62.39; H, 5.57; N, 4.02%.

**{ONNO$^{Me,\ Me}$}AlMe (1).** In a glovebox, the solution of proligand **L$^1$H$_2$** (0.477 g, 1.00 mmol) in 5 mL of toluene was added slowly to a solution of AlMe$_3$ (0.50 mL, 2.0 M in toluene, 1.00 mmol) at room

temperature. Then the mixture was taken out of the glovebox and stirred in a 110 °C oil bath for 48 h. All of the volatiles were removed under vacuum. The resultant yellow solids were recrystallized with a mixture of toluene and *n*-hexane at room temperature to afford yellow crystalline solids in 69% yield (0.356 g). $^1$H NMR ($C_6D_6$, 400 MHz, 298 K): δ 7.82 (br s, 1H, N=C*H*), 7.75 (br s, 1H, N=C*H*), 7.01–6.68 (m, 7H, Ar*H*), 6.31 (br, 3H, Ar*H*), 2.51 (s, 6H, ArC$H_3$), 1.98 (s, 6H, ArC$H_3$), 1.95 (br s, 3H, ArC$H_3$), 1.85 (br s, 3H, ArC$H_3$), –0.54 (s, 3H, AlC$H_3$). $^{13}$C NMR ($C_6D_6$, 100 MHz, 298 K): δ 136.9, 130.9, 129.3, 128.6, 128.5, 125.6 (all Ar*C*), 21.4 (Ar$CH_3$), 20.2 (Ar$CH_3$), 19.6 (Ar$CH_3$), 16.6 (Ar$CH_3$) (due to the broadening of signals, only partial carbon signals could be observed). Anal. Calcd. for: $C_{33}H_{33}AlO_2N_2$·0.41 $C_7H_8$: C, 77.71; H, 6.60; N, 5.05. Found: C, 77.74; H, 6.76; N, 4.92%.

**{ONNO$^{tBu,\ Me}$}AlMe (2).** Following a procedure similar to that described for **1**, **L$^2$H$_2$** (0.561 g, 1.00 mmol) in 5 mL of toluene was treated with a solution of $AlMe_3$ (0.50 mL, 2.0 M in toluene, 1.00 mmol) to give yellow solids after workup. Yellow crystals could be obtained after recrystallization with a mixture of toluene and *n*-hexane at room temperature in 63% yield (0.380 g). $^1$H NMR ($C_6D_6$, 400 MHz, 298 K): δ 7.78 (s, 1H, N=C*H*), 7.72 (s, 1H, N=C*H*), 7.33 (s, 1H, Ar*H*), 7.27 (s, 1H, Ar*H*), 7.01–6.95 (m, 1H, Ar*H*), 6.88 (d, 1H, *J* = 7.2 Hz, Ar*H*), 6.83 (d, 1H, *J* = 7.2 Hz, Ar*H*), 6.73–6.64 (m, 2H, Ar*H*), 6.35 (s, 1H, Ar*H*), 6.32 (s, 1H, Ar*H*), 6.25 (d, 1H, *J* = 6.8 Hz, Ar*H*), 2.08 (s, 3H, ArC$H_3$), 2.04 (s, 3H, ArC$H_3$), 1.98 (s, 3H, ArC$H_3$), 1.80 (s with shoulder, 12H, ArC$H_3$, C(C$H_3$)$_3$), 1.71 (s, 9H, C(C$H_3$)$_3$), –0.55 (s, 3H, AlC$H_3$). $^{13}$C NMR ($C_6D_6$, 100 MHz, 298 K): δ 171.4 (Ar*C*=N), 167.7 (Ar*C*=N), 166.2, 162.4, 148.3, 148.2, 141.9, 141.5, 137.0, 136.9, 135.7, 134.3, 131.8, 131.5, 131.2, 130.9, 129.1, 128.7, 128.5, 124.9, 124.0, 123.8, 122.5, 120.4, 119.5 (all Ar*C*), 35.6 (*C*(CH$_3$)$_3$), 30.0 (C(*C*H$_3$)$_3$), 29.9 (C(*C*H$_3$)$_3$), 20.6 (Ar*C*H$_3$), 20.5 (Ar*C*H$_3$), 19.6 (Ar*C*H$_3$), –8.0 (br, Al*C*H$_3$). $^{27}$Al NMR ($CDCl_3$, 130.3 MHz, 298 K): δ 74 ($w_{1/2}$ = 2398 Hz). Anal. Calcd. for: $C_{39}H_{45}AlO_2N_2$: C, 77.97; H, 7.55; N, 4.66. Found: C, 77.74; H, 7.43; N, 4.75%.

**{ONNO$^{cumyl,\ cumyl}$}AlMe (3).** Following a procedure similar to that described for **1**, **L$^3$H$_2$** (0.893 g, 1.00 mmol) in 5 mL of toluene was treated with a solution of $AlMe_3$ (0.50 mL, 2.0 M in toluene, 1.00 mmol) to give yellow solids after workup. Yellow crystals could be obtained after recrystallization with a mixture of toluene and *n*-hexane at room temperature in 58% yield (0.540 g). $^1$H NMR ($C_6D_6$, 400 MHz, 298 K): δ 7.83 (s, 1H, N=C*H*), 7.62 (s, 1H, N=C*H*), 7.38–7.24 (m, 7H, Ar*H*), 7.18–6.97 (m, 15H, Ar*H*), 6.95–6.90 (m, 1H, Ar*H*), 6.78 (d, 1H, *J* = 8.0 Hz, Ar*H*), 6.71 (br s, 4H, Ar*H*), 6.58 (d, 1H, *J* = 8.0 Hz, Ar*H*), 6.19 (d, 1H, *J* = 7.6 Hz, Ar*H*), 2.19 (s, 3H, ArC$H_3$), 2.08 (s, 3H, ArC$H_3$), 1.91 (s, 6H, cumyl-C$H_3$), 1.85 (s, 3H, cumyl-C$H_3$), 1.69 (s, 3H, cumyl-C$H_3$), 1.45 (s, 6H, cumyl-C$H_3$), 1.44 (s, 6H, cumyl-C$H_3$), –0.97 (s, 3H, AlC$H_3$). $^{13}$C NMR ($C_6D_6$, 100 MHz, 298 K): δ 171.4 (Ar*C*=N), 166.6 (Ar*C*=N), 166.0, 161.9, 151.1, 151.0, 150.8, 147.94, 147.87, 141.4, 138.1, 136.9, 136.8, 136.4, 134.0, 131.0, 130.7, 129.7, 129.4, 129.3, 127.3, 127.1, 126.9, 125.9, 125.6, 125.0, 124.4, 122.4, 119.6, 119.3 (all Ar*C*), 43.4 (*C*Me$_2$Ph), 42.4 (*C*Me$_2$Ph), 31.0 (cumyl-*C*H$_3$), 30.9 (cumyl-*C*H$_3$), 30.8 (cumyl-*C*H$_3$), 30.7 (cumyl-*C*H$_3$), 28.7 (cumyl-*C*H$_3$), 27.4 (cumyl-*C*H$_3$), 19.6 (Ar*C*H$_3$), –7.8 (br, Al*C*H$_3$). Anal. Calcd. for: $C_{64}H_{64}AlO_2N_2$: C, 83.54; H, 7.01; N, 3.04. Found: C, 83.18; H, 7.16; N, 3.06 %.

**{ONNO$^{Me,\ Me}$}Al$_2$Me$_4$ (4).** Following a procedure similar to that described for **1**, **L$^1$H$_2$** (0.477 g, 1.00 mmol) in 5 mL of toluene was treated with a solution of $AlMe_3$ (1.00 mL, 2.0 M in toluene, 2.00 mmol) to give yellow solids after workup. Yellow crystals could be obtained after recrystallization with a mixture of toluene and *n*-hexane at room temperature in 70% yield (0.410 g). $^1$H NMR ($C_6D_6$, 400 MHz, 298 K): δ 7.57 (s, 2H, N=C*H*), 6.90–6.87 (m, 4H, Ar*H*), 6.85 (t, 2H, *J* = 7.6 Hz, Ar*H*), 6.63 (dd, 2H, $J_1$ = 7.6 Hz, $J_2$ = 1.2 Hz, Ar*H*), 6.31 (d, 2H, *J* = 1.2 Hz, Ar*H*), 2.27 (s, 6H, ArC$H_3$), 1.98 (s, 6H, ArC$H_3$), 1.90 (s, 6H, ArC$H_3$), –0.51 (s, 6H, AlC$H_3$), –0.80 (s, 6H, AlC$H_3$). $^{13}$C NMR ($C_6D_6$, 100 MHz, 298 K): δ 172.8 (Ar*C*=N), 162.2, 146.6, 140.4, 140.2, 133.3, 130.5, 130.2, 130.0, 129.8, 125.9, 124.4, 118.6 (all Ar*C*), 20.5 (Ar*C*H$_3$), 20.2 (Ar*C*H$_3$), 16.3 (Ar*C*H$_3$), –8.79 (Al*C*H$_3$), –9.27 (Al*C*H$_3$). Anal. Calcd. for: $C_{36}H_{42}Al_2O_2N_2$: C, 73.45; H, 7.19; N, 4.76. Found: C, 73.28; H, 7.19; N, 4.84%.

**{ONNO$^{tBu,\ Me}$}Al$_2$Me$_4$ (5).** Following a procedure similar to that described for **1**, **L$^2$H$_2$** (0.561 g, 1.00 mmol) in 5 mL of toluene was treated with a solution of $AlMe_3$ (1.00 mL, 2.0 M in toluene, 2.00 mmol) to give yellow solids after workup. Yellow crystals could be obtained after recrystallization with a mixture of toluene and *n*-hexane at room temperature in 74% yield (0.495 g). $^1$H NMR ($C_6D_6$, 400 MHz, 298 K): δ 7.71 (s, 2H, N=C*H*), 7.27 (d, 2H, *J* = 2.2 Hz, Ar*H*), 6.91–6.85 (m, 4H, Ar*H*), 6.51 (dd, 2H, $J_1$ = 7.1 Hz, $J_2$ = 1.9 Hz, Ar*H*), 6.25 (d, 2H, *J* = 2.2 Hz, Ar*H*), 1.99 (s, 6H, ArC$H_3$), 1.91 (s, 6H, ArC$H_3$), 1.53 (s, 18H, C(C$H_3$)$_3$), –0.48 (s, 6H, AlC$H_3$), –0.91 (s, 6H, AlC$H_3$). $^{13}$C NMR ($C_6D_6$, 100 MHz, 298 K): δ 173.4 (Ar*C*=N), 162.8, 147.2, 141.1, 140.0, 136.8, 133.7, 130.6, 130.2, 129.9, 125.7, 124.5, 119.8 (all Ar*C*), 35.2 (*C*(CH$_3$)$_3$), 29.6 (C(*C*H$_3$)$_3$), 20.4 (Ar*C*H$_3$), –9.40 (Al*C*H$_3$), –9.49 (Al*C*H$_3$). $^{27}$Al NMR ($CDCl_3$, 130.3 MHz, 298 K): δ 72 ($w_{1/2}$ = 1728 Hz). Anal. Calcd. for: $C_{42}H_{54}Al_2O_2N_2$: C, 74.97; H, 8.09; N, 4.16. Found: C, 74.71; H, 7.93; N, 4.12%.

**{ONNO$^{cumyl,\ cumyl}$}Al$_2$Me$_4$ (6).** Following a procedure similar to that described for **1**, **L$^3$H$_2$** (0.894 g, 1.00 mmol) in 5 mL of toluene was treated with a solution of $AlMe_3$ (1.00 mL, 2.0 M in toluene, 2.00 mmol) to give yellow solids after workup. Yellow crystals could be obtained after recrystallization with a mixture of toluene and *n*-hexane at room temperature in 72% yield (0.720 g). $^1$H NMR ($C_6D_6$, 400 MHz, 298 K): δ 7.65 (s, 2H, N=C*H*), 7.57 (d, 2H, *J* = 2.4 Hz, Ar*H*), 7.27–7.21 (m, 12H, Ar*H*), 7.19 (m, 2H, Ar*H*), 7.16 (s, 4H, Ar*H*), 7.01 (m, 2H, Ar*H*), 6.89 (d, 2H, *J* = 7.8 Hz, Ar*H*), 6.77 (t, 2H, *J* = 7.8 Hz, Ar*H*), 6.68 (d, 2H, *J* = 2.4 Hz, Ar*H*), 6.59 (d, 2H, *J* = 7.8 Hz, Ar*H*), 1.66 (s, 6H, ArC$H_3$), 1.65 (s, 6H, cumyl-C$H_3$), 1.63 (s, 12H, cumyl-C$H_3$), 1.60 (s, 6H, cumyl-C$H_3$), –0.746 (s, 6H, AlC$H_3$), –0.751 (s, 6H, AlC$H_3$). $^{13}$C NMR ($C_6D_6$, 100 MHz, 298 K): δ 172.0 (Ar*C*=N), 162.4, 150.7, 150.6, 146.3, 141.4, 138.9, 138.5, 137.9, 135.0, 131.1, 130.1, 129.7, 129.3, 128.57, 128.55, 127.0, 126.2, 126.0, 125.7, 125.4, 123.7, 119.1 (all Ar*C*), 42.6 (*C*Me$_2$Ph), 42.4 (*C*Me$_2$Ph), 31.1 (cumyl-*C*H$_3$), 30.9 (cumyl-*C*H$_3$), 29.7 (cumyl-*C*H$_3$), 28.6 (cumyl-*C*H$_3$), 20.4 (Ar*C*H$_3$), –8.54 (Al*C*H$_3$), –9.02 (Al*C*H$_3$). Anal. Calcd. for: $C_{68}Al_2H_{74}O_2N_2$: C, 81.24; H, 7.42; N, 2.79. Found: C, 81.62; H, 7.61; N, 2.51%.

**{ONNO$^{Br,\ tBu}$}Al$_2$Me$_4$ (7).** Following a procedure similar to that described for **1**, **L$^4$H$_2$** (0.690 g, 1.00 mmol) in 5 mL of toluene was treated with a solution of $AlMe_3$ (1.00 mL, 2.0 M in toluene, 2.00 mmol) to give yellow solids after workup. Yellow crystals could be obtained after recrystallization with a mixture of toluene and *n*-hexane twice at room temperature in 10% yield (0.080 g). $^1$H NMR ($C_6D_6$, 400 MHz, 298 K): δ 7.84 (d, 2H, *J* = 2.4 Hz, Ar*H*), 7.36 (s, 2H, N=C*H*), 7.01 (d, 2H, *J* = 2.4 Hz, Ar*H*), 6.79–6.75 (m, 2H, Ar*H*), 6.74 (t, 2H, *J* = 7.6 Hz, Ar*H*), 6.56 (d, 2H, *J* = 7.6 Hz, Ar*H*), 1.78 (s, 6H, ArC$H_3$),

1.18 (s, 18H, C(C$H_3$)$_3$), –0.58 (s, 6H, AlC$H_3$), –0.71 (s, 6H, AlC$H_3$). $^{13}$C NMR ($C_6D_6$, 100 MHz, 298 K): δ 172.1 (Ar*C*=N), 158.9, 145.2, 141.7, 140.4, 139.0, 132.2, 130.2, 129.7, 129.3, 123.6, 119.9, 116.4 (all Ar*C*), 34.0 (*C*(CH$_3$)$_3$), 31.2 (C(*C*H$_3$)$_3$), 20.3 (ArCH$_3$), –8.83 (Al*C*H$_3$), –9.57 (Al*C*H$_3$). Anal. Calcd. for: $C_{40}H_{48}Al_2Br_2O_2N_2$: C, 59.86; H, 6.03; N, 3.49. Found: C, 59.65; H, 6.05; N, 3.53%.

**{ONNO$^{tBu,\ Me}$}Al(O$^i$Pr) (8).** In a glovebox, the solution of proligand **L$^2$H$_2$** (0.561 g, 1.00 mmol) in 5 mL of toluene was added slowly to a solution of AlMe$_3$ (0.50 mL, 2.0 M in toluene, 1.00 mmol) at room temperature. Then the mixture was taken out of the glovebox and stirred in a 110 °C oil bath for 48 h. A solution of $^i$PrOH (60.0 mg, 1.00 mmol) in 2 mL of toluene was added to the above reaction mixture at room temperature and stirred in a 60 °C oil bath for 12 h. All of the volatiles were removed under vacuum. The resultant yellow solids were recrystallized with *n*-hexane at room temperature to afford yellow crystalline solids in 58% yield (0.372 g). $^1$H NMR ($C_6D_6$, 400 MHz, 298 K): δ 7.85 (s, 1H, N=C*H*), 7.72 (s, 1H, N=C*H*), 7.37 (d, 1 H, *J* = 2.0 Hz, Ar*H*), 7.28 (d, 1H, *J* = 7.6 Hz, Ar*H*), 7.24 (d, 1 H, *J* = 2.0 Hz, Ar*H*), 7.15 (t, 1H, *J* = 7.6 Hz, Ar*H*, overlapped with $C_6D_6$ signal), 6.98 (d, 1H, *J* = 7.6 Hz, Ar*H*), 6.72 (d, 1H, *J* = 7.6 Hz, Ar*H*), 6.64 (t, 1H, *J* = 7.6 Hz, Ar*H*), 6.39 (s, 1H, Ar*H*), 6.29 (s, 1H, Ar*H*), 6.18 (d, 1H, *J* = 7.6 Hz, Ar*H*), 3.98 (m, 1H, OC*H*(CH$_3$)$_2$), 2.08 (s, 3H, ArC*H*$_3$), 2.03 (s, 3H, ArC*H*$_3$), 2.00 (s, 3H, ArC*H*$_3$), 1.89 (s, 3H, ArC*H*$_3$), 1.81 (s, 9H, C(C*H*$_3$)$_3$), 1.77 (s, 9H, C(C*H*$_3$)$_3$), 1.25 (br s, 3H, OCH(C*H*$_3$)$_2$), 0.51 (br s, 3H, OCH(C*H*$_3$)$_2$). $^{13}$C NMR ($C_6D_6$, 100 MHz, 298 K): δ 171.4 (Ar*C*=N), 167.2 (Ar*C*=N), 166.6, 162.3, 148.9, 148.6, 141.3, 141.1, 137.1, 136.3, 136.0, 134.0, 131.7, 131.6, 131.5, 129.9, 129.2, 128.6, 125.0, 124.7, 124.2, 123.8, 119.9, 119.3 (all Ar*C*), 63.1 (O*C*H(CH$_3$)$_2$), 35.9 (*C*(CH$_3$)$_3$), 35.7 (*C*(CH$_3$)$_3$), 30.2 (C(*C*H$_3$)$_3$), 29.9 (C(*C*H$_3$)$_3$), 20.7 (OCH(*C*H$_3$)$_2$), 20.5 (OCH(*C*H$_3$)$_2$), 19.8 (Ar*C*H$_3$), 19.6 (Ar*C*H$_3$). Anal. Calcd. For $C_{41}H_{49}AlN_2O_3$: C, 76.37; H, 7.66; N, 4.34. Found: C, 75.67; H, 7.75; N, 4.37%.

**{ONNO$^{tBu,\ Me}$}Al(OBn) (9).** Following a procedure similar to that described for **8**, a solution of BnOH (108.0 mg, 1.00 mmol) was added instead. After workup, the resultant yellow solids were recrystallized with toluene at room temperature to afford yellow crystalline solids in 61% yield (0.420 g). $^1$H NMR ($C_6D_6$, 400 MHz, 298 K): δ 7.76 (s, 2H, N=C*H*), 7.30 (s, 1H, Ar*H*), 7.27 (s, 1H, Ar*H*), 7.15 (s,1H, Ar*H*, overlapped with $C_6D_6$ signal), 7.03–6.96 (m, 5H, Ar*H*), 6.92 (d, 2H, *J* = 6.4 Hz, Ar*H*), 6.73 (d, 1H, *J* = 7.6 Hz, Ar*H*), 6.65 (t, 1H, *J* = 7.6 Hz, Ar*H*), 6.33 (s, 1H, Ar*H*), 6.17 (s, 1H, Ar*H*), 6.16 (d, 1H, *J* = 7.6 Hz, Ar*H*), 4.81–4.65 (m, 2H, OC*H*$_2$Ph), 2.07 (s, 3H, ArC*H*$_3$), 2.04 (s, 3H, ArC*H*$_3$), 2.02 (s, 3H, ArC*H*$_3$), 1.89 (s, 3H, ArC*H*$_3$), 1.78 (s, 9H, C(C*H*$_3$)$_3$), 1.73 (s, 9H, C(C*H*$_3$)$_3$). $^{13}$C NMR ($C_6D_6$, 100 MHz, 298 K): δ 171.7 (Ar*C*=N), 167.6 (Ar*C*=N), 166.4, 162.3, 148.8, 148.4, 147.0, 141.3, 140.9, 137.2, 136.14, 136.11, 134.2, 131.8, 131.6, 130.0, 129.3, 128.9, 128.7, 127.6, 126.2, 125.3, 125.2, 124.3, 124.2, 123.9, 120.0, 119.4 (all Ar*C*), 66.2 (OC*H*$_2$Ph), 35.8 (*C*(CH$_3$)$_3$), 35.7 (*C*(CH$_3$)$_3$), 30.3 (C(*C*H$_3$)$_3$), 30.0 (C(*C*H$_3$)$_3$), 20.6 (Ar*C*H$_3$), 20.5 (Ar*C*H$_3$), 19.8 (Ar*C*H$_3$), 19.6 (Ar*C*H$_3$). Anal. Calcd. for: $C_{45}H_{49}AlN_2O_3$: C, 78.01; H, 7.13; N, 4.04. Found: C, 77.36; H, 7.10; N, 4.06%.

**{ONNO$^{tBu,\ Me}$}Al(OCMe$_2$CO$_2$Me) (10).** Following a procedure similar to that described for **8**, a solution of methyl 2-hydroxybutyrate (118.0 mg, 1.00 mmol) was added. After workup, the resultant yellow solids were recrystallized with *n*-hexane at room temperature to afford yellow crystalline solids in 42 % yield (0.293 g). $^1$H NMR ($C_6D_6$, 400 MHz, 298 K): δ 7.88 (s, 1H, N=C*H*), 7.87 (s, 1H, N=C*H*), 7.34 (d, 1H, *J* = 1.6 Hz, Ar*H*), 7.26 (d, 1H, *J* = 1.6 Hz, Ar*H*), 7.05 (t, 1H, *J* = 7.6 Hz, Ar*H*), 6.96 (d, 1H, *J* = 7.6 Hz, Ar*H*), 6.91 (d, 1H, *J* = 7.6 Hz, Ar*H*), 6.78 (t, 1H, *J* = 7.6 Hz, Ar*H*), 6.67 (d, 1H, *J* = 7.6 Hz, Ar*H*), 6.59 (s, 1H, Ar*H*), 6.48 (s, 1H, Ar*H*), 6.46 (d, 1H, *J* = 7.6 Hz, Ar*H*), 3.06 (s, 3H, COOC*H*$_3$), 2.18 (s, 3H, ArC*H*$_3$), 2.05 (s, 3H, ArC*H*$_3$), 2.01 (s, 3H, ArC*H*$_3$), 1.84 (s, 9H, C(C*H*$_3$)$_3$), 1.80 (s, 3H, ArC*H*$_3$), 1.69 (s, 9H, C(C*H*$_3$)$_3$), 1.29 (s, 3H, OC(C*H*$_3$)$_2$), 1.05 (s, 3H, OC(C*H*$_3$)$_2$). $^{13}$C NMR ($C_6D_6$, 100 MHz, 298 K): δ 193.6 (*C*OO), 168.7 (Ar*C*=N), 168.0 (Ar*C*=N), 166.0, 164.9, 150.8, 149.9, 141.7, 140.2, 137.3, 136.6, 134.2, 133.8, 132.3, 131.7, 131.4, 131.3, 128.5, 127.6, 127.5, 124.5, 123.1, 122.5, 121.5, 121.4, 119.4, 118.7, 110.5 (all Ar*C*), 72.5 (O*C*(CH$_3$)$_2$), 54.2 (COO*C*H$_3$), 35.7 (*C*(CH$_3$)$_3$), 31.0 (C(*C*H$_3$)$_3$), 30.6 (C(*C*H$_3$)$_3$), 30.3 (OC(*C*H$_3$)$_2$), 28.4 (OC(*C*H$_3$)$_2$), 20.72 (Ar*C*H$_3$), 20.66 (Ar*C*H$_3$), 20.0 (Ar*C*H$_3$), 19.9 (Ar*C*H$_3$). $^{27}$Al NMR ($CDCl_3$, 130.3 MHz, 298 K): δ 70 ($w_{1/2}$ = 2657 Hz), 35 ($w_{1/2}$ = 2731 Hz). Anal. Calcd. For $C_{43}H_{51}AlN_2O_5$·(0.2 $C_6H_{14}$): C, 73.75; H, 7.91; N, 3.81. Found: C, 74.24; H, 7.94; N, 3.66%.

**{ONNO$^{tBu,\ Me}$}Al[(*S*)-OCHMeCO$_2$Me] (11).** Following a procedure similar to that described for **8**, a solution of methyl (*S*)-lactate (108.0 mg, 1.00 mmol) was added. After workup, the resultant yellow solids were recrystallized with *n*-hexane at room temperature to afford yellow crystalline solids in 39% yield (0.267 g). $^1$H NMR ($C_6D_6$, 400 MHz, 298 K): δ 7.87 (s, 1H, N=C*H*), 7.83 (s, 1H, N=C*H*), 7.82 (s, 1H, N=C*H*), 7.78 (s, 1H, N=C*H*), 7.34 (s, 2H, Ar*H*), 7.24 (s, 2H, Ar*H*), 7.02 (d, 1H, *J* = 2.0 Hz, Ar*H*), 7.00 (d, 1H, *J* = 2.0 Hz, Ar*H*), 6.97–6.91 (m, 3H, Ar*H*), 6.83 (d, 1H, *J* = 7.6 Hz, Ar*H*), 6.78 (d, 1H, *J* = 7.6 Hz, Ar*H*), 6.74 (d, 1H, *J* = 7.6 Hz, Ar*H*), 6.70 (d, 2H, *J* = 7.2 Hz, Ar*H*), 6.56 (d, 2H, *J* = 7.2 Hz, Ar*H*), 6.47 (d, 1H, *J* = 7.6 Hz, Ar*H*), 6.45 (s, 3H, Ar*H*), 4.48 (q, 1H, *J* = 6.8 Hz, OC*H*(CH$_3$)$_2$), 4.30 (q, 1H, *J* = 6.8 Hz, OC*H*(CH$_3$)$_2$), 3.06 (s, 3H, COOC*H*$_3$), 2.90 (s, 3H, COOC*H*$_3$), 2.17 (s, 3H, ArC*H*$_3$), 2.15 (s, 3H, ArC*H*$_3$), 2.03 (s, 3H, ArC*H*$_3$), 1.84 (s, 3H, ArC*H*$_3$), 1.81 (s, 18H, C(C*H*$_3$)$_3$), 1.71 (s, 9H, C(C*H*$_3$)$_3$), 1.69 (s, 9H, C(C*H*$_3$)$_3$), 1.17 (d, 3H, *J* = 6.8 Hz, OCHC*H*$_3$), 1.16 (d, 3H, *J* = 6.8 Hz, OCHC*H*$_3$). $^{13}$C NMR ($C_6D_6$, 100 MHz, 298 K): δ 189.8 (*C*OO), 189.0 (*C*OO), 169.7, 169.4, 167.7, 167.5 (Ar*C*=N), 165.73, 165.69, 164.8, 150.4, 150.1, 150.0, 149.6, 141.58, 141.55, 140.6, 137.4, 137.0, 136.8, 136.7, 134.6, 134.3, 133.9, 132.4, 132.1, 131.6, 131.5, 131.4, 131.3, 128.7, 128.5, 127.6, 127.5, 124.2, 124.0, 123.5, 123.3, 122.9, 122.6, 122.0, 121.28, 121.23, 119.7, 119.5, 119.4, 110.4 (all Ar*C*), 69.4, 68.4 (O*C*HCH$_3$), 53.6, 53.4 (COO*C*H$_3$), 35.65, 35.60, 35.57 (*C*(CH$_3$)$_3$), 30.3, 30.19, 30.16, 30.1 (C(*C*H$_3$)$_3$), 21.7, 21.5 (OCH*C*H$_3$), 20.74, 20.70, 20.6, 19.92, 19.91 (Ar*C*H$_3$). $^{27}$Al NMR ($CDCl_3$, 130.3 MHz, 298 K): δ 69 ($w_{1/2}$ = 1548 Hz), 36 ($w_{1/2}$ = 2740 Hz). Anal. Calcd. For $C_{42}H_{49}AlN_2O_5$·(0.5 $C_6H_{14}$&0.2 $C_7H_9$): C, 74.27; H, 7.74; N, 3.73. Found: C, 74.10; H, 7.74; N, 3.71%.

**Typical polymerization procedures**

In a Braun Labstar glovebox, an initiator solution from a stock solution in toluene was injected sequentially into a series of 10 mL Schlenk tube loaded with *rac*-LA and suitable amounts of dry solvent. Then each Schlenk tube was taken out of the glovebox and immerged into a 110 °C oil bath. After specified time intervals, the reaction mixture was quenched by adding excess amount of wet petroleum ether, and then dissolved in dichloromethane. All of the volatiles in the aliquots were removed, and the residue was subjected to monomer conversion determination, which was monitored by integrating monomer versus polymer methine

resonances in $^1$H NMR spectrum ($CDCl_3$, 400 MHz, 298 K). The precipitates collected from the bulk mixture were dried in air, dissolved with dichloromethane, and sequentially precipitated into methanol. The obtained polymer was further dried in a vacuum oven at 60 °C for 16 h. Each reaction was used as one data point. In the cases where $^i$PrOH was used, the solution of initiator was injected into the solution of *rac*-LA and $^i$PrOH in toluene. Otherwise, the procedures were the same.

**Oligomerization Experiment**

Oligomerization of *rac*-LA was carried out in toluene at 110 °C with complex **8** as the initiator under the condition of [*rac*-LA]:[**8**] = 20:1. The reaction mixture was stirred for 24 h, the mixture was then quenched by adding wet petroleum ether. The precipitated oligomers were collected, dried under vacuum, and used for $^1$H NMR and ESI-TOF MS analysis.

**X-ray Crystallography**

Singe crystals suitable for X-ray analysis were obtained from a saturated ethanol solution for proligand $\mathbf{L^2H_2}$ or from saturated toluene/*n*-hexane solutions for complexes **1**-**3**, **6**, **8**-**11** at room temperature. Diffraction data were collected on a Bruker SMART APEX II diffractometer with graphite-monochromated Mo-Kα (λ = 0.71073 Å) radiation. All data were collected at about 130 K or 140 K using the ω-scan techniques. All structures were solved by direct methods and refined using Fourier techniques. An absorption correction based on *SADABS* was applied.[34] All non-hydrogen atoms were refined by full-matrix least squares on $F^2$ using the *SHELXTL* program package.[35] Hydrogen atoms were located and refined by the geometry method. Cell refinement, data collection, and reduction were done by Bruker *SAINT*.[36] Structure solution and refinement were performed by *SHELXS-97*[37] and *SHELXL-97*,[38] respectively. Crystal data and details of data collection and structure refinement for the different compounds are given in Tables S1-S4. The crystallographic data (excluding structure factors) are available as Supporting Information, as CIF files.

## Acknowledgements

This work is subsidized by the National Natural Science Foundation of China (NNSFC, 21074032 and 21474028), the Program for New Century Excellent Talents in University (for H. Ma, NCET-06-0413) and the Fundamental Research Funds for the Central Universities (WD1113011). All the financial supports are grate fully acknowledged. H. Ma also thanks the very kind donation of a Braun glove-box by AvH foundation.

## Notes and references

1 (*a*) K. E. Uhrich, S. M. Cannizzaro, R. S. Langer and K. M. Shakesheff, *Chem. Rev.*, 1999, **99**, 3181−3198; (*b*) D. J. Mooney, G. Organ, J. P. Vacanti and R. S. Langer, *Cell Transplant*, 1994, **2**, 203−209; (*c*) J. L. Eguiburu, M. J. Fernandez-Berridi, F. P. Cossio and J. S. Roman, *Macromolecules*, 1999, **32**, 8252−8258.

2 (*a*) M. S. Reeve, S. P. Mccarthy, M. J. Downey and R. A. Gross, *Macromolecules*, 1994, **27**, 825−831; (*b*) J. R. Sarasua, R. E. Prud'homme, M. Wisniewski, A. Le Borgne and N. Spassky, *Macromolecules*, 1998, **31**, 3895−3905.

3 X. C. Zhang, M. F. A. Goosen, U. P. Wyss and D. Pichora, *J. Macromol. Sci. Rev. Macromol. Chem. Phys.*, 1993, **C33**, 81−102.

4 (*a*) K. Fukushima, Y. Kimura, *Polym. Int.*, 2006, **55**, 626−642; (*b*) M. H. Chisholm, N. J. Patmore and Z. Zhou, *Chem. Commun.*, 2005, 127−129.

5 (*a*) M. J. Stanford and A. P. Dove, *Chem. Soc. Rev.*, 2010, **39**, 486–494; (*b*) P. J. Dijkstra, H. Du and J. Feijen, *Polym. Chem.*, 2011, **2**, 520–527.

6 (*a*) N. Spassky, M. Wisniewski, C. Pluta and A. LeBorgne, *Macromol. Chem. Phys.*, 1996, **197**, 2627−2637; (*b*) C. Radano, G. Baker and M. Smith, *J. Am. Chem. Soc.*, 2000, **122**, 1552−1553; (*c*) T. M. Ovitt and G. W. Coates, *J. Am. Chem. Soc.*, 2002, **122**, 1316−1326; (*d*) Z. Zhong, P. J. Dijkstra and J. Feijen, *Angew. Chem. Int. Ed.*, 2002, **41**, 4150−4153; (*e*) Z. Zhong, P. Dijkstra and J. Feijen, *J. Am. Chem. Soc.*, 2003, **125**, 11291−11298; (*f*) K. Majerska and A. Duda, *J. Am. Chem. Soc.*, 2004, **126**, 1026−1027; (*g*) N. Maudoux, T. Roisnel, V. Dorcet, J.-F. Carpentier and Y. Sarazin, *Chem. Eur. J.*, 2014, **20**, 6131–6147; (*h*) A. Pilone, K. Press, I. Goldberg, M. Kol, M. Mazzeo and M. Lamberti, *J. Am. Chem. Soc.,* 2014, **136**, 2940–2943.

7 (*a*) H. Wang and H. Ma, *Chem. Commun.*, 2013, **49**, 8686–8688; (*b*) M. Honrado, A. Otero, J. Fernández-Baeza, L. F. Sánchez-Barba, A. Garcés, A. Lara-Sánchez and A. M. Rodríguez, *Organometallics,* 2013, **32**, 3437–3440; (*c*) M. Honrado, A. Otero, J. Fernández-Baeza, L. F. Sánchez-Barba, A. Garcés, A. Lara-Sánchez and A. M. Rodríguez, *Organometallics,* 2014, **33**, 1859–1866; (*d*) S. Abbina and G. Du, *ACS Macro. Lett.*, 2014, **3**, 689−692; (*e*) Z. Mou, B. Liu, M. Wang, H. Xie, P. Li, L. Li, S. Li and D. Cui, *Chem. Commun.*, 2014, **50**, 11411−11414.

8 (*a*) D. C. Aluthge, B. O. Patrick and P. Mehrkhodavandi, *Chem. Commun.,* 2013, **49**, 4295−4297; (*b*) D. C. Aluthge, J.-M. Ahn and P. Mehrkhodavandi, *Chem. Sci.*, 2015, **6**, 5284–5292; (*c*) D. C. Aluthge, E. X. Yan, J.-M. Ahn and P. Mehrkhodavandi, *Inorg. Chem.*, 2014, **53**, 6828–6836.

9 P. Horeglad, G. Szczepaniak, M. Dranka and J. Zachara, *Chem. Commun.*, 2012, **48**, 1171–1173.

10 (*a*) J. Zhang, J. Xiong, Y. Sun, N. Tang and J. Wu, *Macromolecules,* 2014, **47**, 7789–7796; (*b*) J. Xiong, J. Zhang, Y. Sun, Z. Dai, X. Pan and J. Wu, *Inorg. Chem.*, 2015, **54**, 1737–1743; (*c*) Z. Dai, Y. Sun, J. Xiong, X. Pan and J. Wu, *ACS Macro Lett.*, 2015, **4**, 556−560; (*d*) Y. Sun, J. Xiong, Z. Dai, X. Pan, N. Tang, and Jincai Wu, *Inorg. Chem.*, 2016, **55**, 136−143..

11 S. Fortun, P. Daneshmand, F. Schaper. *Angew. Chem. Int. Ed.*, 2015, **54**, 13669 –13672.

12 (*a*) M. D. Jones, S. L. Hancock, P. McKeown, P. M. Schafer, A. Buchard, L. H. Thomas, M. F. Mahon and J. P. Lowe, *Chem. Commun.*, 2014, **50**, 15967−15970; (*b*) M. D. Jones, L. Brady, P. McKeown, A. Buchard, P. M. Schafer, L. H. Thomas, M. F. Mahon, T. J. Woodman and J. P. Lowe, *Chem. Sci.*, 2015, **6**, 5034–5039.

13 (*a*) P. L. Arnold, J.-C. Buffet, R. P. Blaudeck, S. Sujecki, A. J. Blake and C. Wilson, *Angew. Chem. Int. Ed.*, 2008, **47**, 6033–6036; (*b*) C. Bakewell, T.-P.-A. Cao, N. Long, X. F. Le Goff, A. Auffrant and C. K. Williams, *J. Am. Chem. Soc.*, 2012, **134**, 20577−20580; (*c*) C. Bakewell, A. J. P. White, N. Long and C. K. Williams, *Angew. Chem. Int. Ed.*, 2014, **53**, 9226–9230.

14 P. Hormnientry, E. L. Marshall, V. C. Gibson, R. I. Pugh and A. J. P. White, *PNAS*, 2006, **103**, 15343–15348.

15 (*a*) N. Nomura, R. Ishii, Y. Yamamoto and T. Kondo, *Chem. Eur. J.*, 2007, **13**, 4433–4451; (*b*) Tang, Z.; Pang, X.; Sun, J.; Du, H.; Chen X.; Wang, X. and Jing, X. *J. Polym. Sci. Part A: Polym. Chem.*, 2006, **44**, 4932–4938.

16 (*a*) W. Li, W. Wu, Y. Wang, Y. Yao, Y. Zhang and Q. Shen, *Dalton Trans.*, 2011, **40**, 11378–11381; (*b*) X.-F. Yu and Z.-X. Wang, *Dalton Trans.*, 2013, **42**, 3860–3868; (*c*) H.-L. Han, Y. Liu, J.-Y. Liu, K. Nomura and Y.-S. Li, *Dalton Trans.*, 2013, **42**, 12346–12353; (*d*) S. Sun, K. Nie, Y. Tan, B. Zhao, Y. Zhang, Q. Shen and Y. Yao, *Dalton Trans.*, 2013, **42**, 2870–2878; (*e*) M. Normand, T. Roisnel, J.-F. Carpentier and E. Kirillov, *Chem. Commun.*, 2013, **49**, 11692–11694; (*f*) I. Yu, J. A. Ramírez and P. Mehrkhodavandi, *J. Am. Chem. Soc.*, 2012, **134**, 12758–12773; (g) X. Pang, R. Duan, X. Li, B. Gao, Z. Sun, X. Wang and X. Chen, RSC Adv., 2014, **4**, 22561–22566; (h) C. Romain, C. Fliedel, S. B.-Laponnaz and S. Dagorne, *Organometallics*, 2014, **33**, 5730–5739; (i) L. Li, B. Liu, D. Liu, C. Wu, S. Li, B. Liu and D. Cui, *Organometallics*, 2014, **33**, 6474–6480; (j) L. Chen, W. Li, D. Yuan, Y. Zhang, Q. Shen and Y. Yao, *Inorg. Chem.*, 2015, **54**, 4699–4708.

17 S. Bian, S. Abbina, Z. Lu, E. Kolodka and G. Du, *Organometallics*, 2014, **33**, 2489–2495.

18 M.-A. Munoz-Hernandez, T. S. Keizer, P. Wei, S. Parkin and D. A. Atwood, *Inorg. Chem.*, 2001, **40**, 6782–6787.

19 (*a*) Q. Wang, L. Xiang, H. Song and G. Zi, *Inorg. Chem.*, 2008, **47**, 4319–

4328; (*b*) J. R. Perkins and R. G. Carter, *J. Am. Chem. Soc.*, 2008, **130**, 3290–3291; (*c*) X. Li, X. Meng, H. Su, X. Wu and D. Xu, *Synlett*, 2008, **6**, 857–860.
20 (*a*) J. P. Duxbury, J. N. D. Warne, R. Mushtaq, C. Ward, M. Thornton-Pett, M. Jiang, R. Greatrex and T. P. Kee, *Organometallics*, 2000, **19**, 4445–4457; (*b*) M. A. V. Aelstyn, T. S. Keizer, D. L. Klopotek, S. Liu, M.-A. Munoz-Hernandez, P. Wei and D. A. Atwood, *Organometallics*, 2000, **19**, 1796–1801; (*c*) W. Yao, Y. Mu, A. Gao, W. Gao and L. Ye, *Dalton Trans.*, 2008, 3199–3206.
21 J. S. Klitzke, T. Roisnel, E. Kirillov, O. Casagrande and J.-F. Carpentier, *Organometallics*, 2014, **33**, 309–321.
22 The interconversion of the helicity of the tetradentate ligand wrapping around the metal center will render the two fragments in the same ligand chemically equivalent.
23 (a) X. Pang, H. Du, X. Chen, X. Wang and X. Jing, *Chem. Eur. J.*, 2008, **14**, 3126–3136; (b) H.Du, X. Pang, H. Yu, X. Zhuang, X. Chen, D. Cui, X. Wang and Xiabin Jing, *Macromolecules*, 2007, **40**, 1904–1913; (c) M. O. Miranda, Y. DePorre, H. Vazquez-Lima, M. A. Johnson, D. J. Marell, C. J. Cramer and W.B. Tolman, *Inorg. Chem.*, 2013, **52**, 13692–13701.
24 (*a*) C. K. Williams, L. E. Breyfogle, S. K. Choi, W. Nam, V. G. Young, M. A. Hillmyer and W. B. Tolman, *J. Am. Chem. Soc.*, 2003, **125**, 11350−11359; (*b*) A. Pilone, M. Lamberti, M. Mazzeo, S. Milione and C. Pellecchia, *Dalton Trans.*, 2013, **42**, 13036−13047; (*c*) S.-C. Roşca, D.-A. Rosca, V. Dorcet, C. M. Kozak, F. M. Kerton, J.-F. Carpentier and Y. Sarazin, *Dalton Trans.*, 2013, **42**, 9361−9375.
25 H. Wang, Y. Yang and H. Ma, *Macromolecules*, 2014, **47**, 7750−7764
26 H. Ma and J. Okuda, *Macromolecules*, 2005, **38**, 2665−2673.
27 (*a*) H.-Y. Chen, J. Zhang, C.-C. Lin, J. H. Reibenspies and S. A. Miller, *Green Chem.*, 2007, **9**, 1038–1040; (*b*) B. J. O'Keefe, L. E. Breyfogle, M. A. Hillmyer and William B. Tolman, *J. Am. Chem. Soc.*, 2002, **124**, 4384−4393, (*c*) Y. Yang, H. Wang and H. Ma, *Inorg. Chem.*, 2015, **54**, 5839−5854.
28 (*a*) A. Amgoune, C. M. Thomas and J.-F. Carpentier, *Macromol. Rapid Commun.*, 2007, **28**, 693–697; (*b*) N. Ajellal, J.-F. Carpentier, C. Guillaume, S. M. Guillaume, M. Helou, V. Poirier, Y. Sarazin and A. Trifonov, *Dalton Trans.*, 2010, **39**, 8363–8376; (*c*) M. Helou, O. Miserque, J.-M. Brusson, J.-F. Carpentier and S. M. Guillaume, *Chem. Eur. J.*, 2008, **14**, 8772–8775; (*d*) S. Tabthong, T. Nanok, P. Kongsaeree, S. Prabpai and P. Hormnientry, *Dalton Trans.*, 2014, **43**, 1348–1359.
29 (*a*) L. Clark, M. G. Cushion, H. E. Dyer, A. D. Schwarz, R. Duchateaub and P. Mountford, *Chem. Commun.*, 2010, **46**, 273–275; (*b*) S. Tabthong, T. Nanok, P. Kongsaeree, S. Prabpai and P. Hormnientry, *Dalton Trans.*, 2014, **43**, 1348–1359; (*c*) Y. Sarazin, B. Liu, T. Roisnel, L. Maron and J.-F. Carpentier, *J. Am. Chem. Soc.*, 2011, **133**, 9069–9087; (*d*) Y. Wang, W. Zhao, X. Liu, D. Cui and Y.-X. Chen, *Macromolecules*, 2012, **45**, 6957−6965; (*e*) J. P. MacDonald and M. P. Shaver, *ACS Symp. Ser.*, 2015, **1192**, 147–167.
30 S. Song, X. Zhang, H. Ma, Y. Yang, *Dalton Trans.*, 2012, **41**, 3266−3277.
31 The chiral biphenyl bridged salen ligand in these aluminum complexes is rigid, which shows no fluxional behaviour in a broad temperature range. Therefore, we consider that the site-control mechanism is more suitable for our system.
32 B. M. Chamberlain, M. Cheng, D. R. Moore, T. M. Ovitt, E. B. Lobkovsky and G. W. Coates, *J. Am. Chem. Soc.,* 2001, **123**, 3229−3238.
33 (*a*) P. D. Knight, P. N. O'Shaughnessy, I. J. Munslow, B. S. Kimberley and P. Scott, *J. Organomet. Chem.*, 2003, **683**, 103−113; (*b*) P. D. Knight, G. Clarkson, M. L. Hammond, B. S. Kimberley and P. Scott, *J. Organomet. Chem.*, 2005, **690**, 5125−5144.
34 *SADABS, Bruker Nonius area detector scaling and absorption correction*, version 2.05; Bruker AXS Inc.: Madison, WI, 1996.
35 G. M. Sheldrick, *SHELXTL 5.10 for windows NT, Structure Determination Software Programs*; Bruker AXS Inc.: Madison, WI, 1997.
36 *SAINT*, version 6.02; Bruker AXS Inc.: Madison WI, 1999; 53711−5373.
37 G. M. Sheldrick, *SHELXS-97, Program for the Solution of Crystal Structures*; University of Göttingen: Göttingen, Germany, 1990.
38 G. M. Sheldrick, *SHELXL-97, Program for the Solution of Crystal Structures*; University of Göttingen: Göttingen, Germany, 1990.

**For Table of Contents Only**

# Aluminum Methyl, Alkoxide and α-Alkoxy Ester Complexes Supported by 6,6'-dimethylbiphenyl-bridged Salen Ligands: Synthesis, Characterization and Catalysis for *rac*-Lactide Polymerization

*Chao Kan, Jilei Ge and Haiyan Ma**

Shanghai Key Laboratory of Functional Materials Chemistry and Laboratory of Organometallic Chemistry, East China University of Science and Technology, 130 Meilong Road, Shanghai 200237, P. R. China

A series of mono- and dinuclear aluminum complexes bearing racemic 2,2'-diamino-6,6'-dimethylbiphenyl-bridged salen ligands could efficiently catalyze the ROP of *rac*-LA, producing the isotactic enriched and atactic PLA, respectively. The dissociation of one N donor and the association/dissociation equilibrium of the carbonyl group of α-alkoxy ester ligand was found in the model *O*-lactate mononuclear complexes.